ANALYSIS OF UNSATURATED FLOW BASED ON CHEMICAL TRACERS (CHLORIDE, ^{36}CL, ^{3}H, AND BROMIDE) AND COMPARISON WITH PHYSICAL DATA, CHIHUAHUAN DESERT, TEXAS

Bridget R. Scanlon and Bernd C. Richter

Final Contract Report

Prepared for

Texas Low-Level Radioactive Waste Disposal Authority

under Interagency Contract Number IAC(90-91)0268

by

Bureau of Economic Geology

W. L. Fisher, Director

The University of Texas at Austin

Austin, Texas 78713

July 1990

CONTENTS

Figures

Sounds like a bad play before it starts!

Tables

EXECUTIVE SUMMARY

Three chemical tracer studies have been conducted to evaluate the flux of water in the unsaturated zone beneath the Chihuahuan Desert in West Texas and to compare the results with the flux predicted from physical attributes of the system. First, the spatial variability in soil moisture flux was evaluated from 10 chloride profiles located in ephemeral stream and interstream settings. Second, thermonuclear ^{3}H and ^{36}Cl were measured in an ephemeral stream setting to quantify flux in the shallow unsaturated zone during the past 35 yr. Third, a bromide pulse was applied over a 100-m^2 area, leached by natural precipitation for 1 yr, then recovered and measured in soil cores.

Specific moisture fluxes based on chloride mass balance ranged from 0.01 to 1 mm a^{-1} (4×10^{-4} to 0.04 inches a^{-1}). Specific moisture flux based on the 0.5-m depth of the $^{36}Cl/Cl$ peak was 1.4 mm a^{-1} (0.06 inch a^{-1}), or 0.5% of the mean annual precipitation rate. The $^{36}Cl/Cl$ peak was intensified by repeated alternation of the flux vector from downward (infiltration) to upward (evapotranspiration); therefore, the distribution of ^{36}Cl cannot be simulated with unidirectional water movement. The ^{3}H tracer penetrated much deeper than did the ^{36}Cl tracer, yielding a specific moisture flux of 7 mm a^{-1} (0.3 inch a^{-1}). The deeper penetration of ^{3}H relative to ^{36}Cl is attributed to downward vapor transport controlled by summer temperature gradients.

In contrast to the chemical tracer data that record cumulative downward-directed flux, water potential gradients indicate predominantly upward water movement under isothermal conditions, except in the shallow (1 m [3 ft]) subsurface immediately after precipitation events. In the shallow unsaturated zone where downward- and upward-directed fluxes of liquid and vapor phases occur, interpretation of chemical tracer data is critical for delineating the net movement of water during a long time period.

INTRODUCTION

Thick unsaturated zones in arid regions are being considered as potential sites for radioactive waste disposal facilities because of low recharge potentials that result from low precipitation and high evapotranspiration rates, and because the low permeability of a thick unsaturated zone may provide a natural barrier to radionuclide migration to the water table. Both physical and chemical methods are used to evaluate water movement in the unsaturated zone. In general, physical approaches furnish information on potential gradients that affect flow during the monitoring period. In arid regions, several potential gradients, such as water (matric and osmotic) potential, temperature, and gravitational potential, may be operative, but it is often difficult to assess the relative importance of each in controlling flow. In addition, highly nonlinear relationships between water content, water potential, and hydraulic conductivity in extremely dry unsaturated systems result in large uncertainties in estimates of flow velocities.

Chemical methods generally use the distribution of environmental or applied tracers such as ionic bromide and chloride and radioactive isotopes such as chlorine-36 (^{36}Cl) and tritium (^{3}H) to determine the rate of water flow in the unsaturated zone. Because the distributions of these tracers record movement of fluid during a much longer time period (30 to 24,000 yr) than that considered in the physical studies, chemical tracer data are of critical importance in the prediction of flow beneath radioactive waste disposal sites. Chemical tracers also provide information on net movement of water that is difficult to evaluate from physical data because of repeated alternation between infiltration and evapotranspiration in the shallow unsaturated zone.

The unsaturated zone in the Hueco Bolson, within the Chihuahuan Desert in West Texas, is being considered as a potential repository for disposal of low-level radioactive waste (Fig. 1). Hueco Bolson is part of the Rio Grande Rift and formed as a result of Basin and Range deformation during the Tertiary (Gustavson, 1990). The unsaturated zone consists of 0 to 15 m (0 to 49 ft) of silty to gravelly loam of the Tertiary and Quaternary Camp Rice Formation, underlain

by approximately 140 m (460 ft) of clay with interbedded silt and sand of the upper Tertiary Fort Hancock Formation. Sediments were deposited in lacustrine, alluvial, and eolian environments (Gustavson, 1990). The present surface of the Hueco Bolson is an alluvial plain sloping 1–1.5% toward the Rio Grande. Modern ephemeral streams that drain the alluvial plain lack well-defined channels in their headwaters. The upper reaches of the ephemeral streams drain into incised channels (arroyos) southwest of the study area (Fig. 1). Shrubs, such as creosote and mesquite, are common and root to depths of 1 to 5 m (3 to 16 ft). The regional climate is subtropical arid (Larkin and Bomar, 1983); mean annual precipitation is 280 mm (11 inches) and has large inter-annual variations that range from 110 to 440 mm (4 to 17 inches) in El Paso (Fig. 2). Approximately 60% of the precipitation falls between June 1 and September 30. Potential evapotranspiration (Class A pan) is as much as 7 times mean annual precipitation.

The objective of this study was to determine the direction and rate of water movement in the upper part of the unsaturated zone of the Hueco Bolson. This paper focuses on chemical methods of analyzing water movement based on the distribution of environmental and applied tracers. Key components of the research include (1) evaluation of the spatial variability in moisture fluxes based on chloride mass balance, (2) comparison of flux estimates from chloride, $^{36}Cl/Cl$, and ^{3}H, (3) comparison of moisture fluxes at Hueco Bolson with those from other arid regions, and (4) comparison of fluxes predicted by chemical and physical data.

A detailed account of the physical hydrology of the unsaturated zone is presented in Scanlon and others (1990). Because some of these hydrologic data will be compared with the chemical tracer data, the major findings of the physical flow studies are summarized here. Physical data indicate that most water movement is in the uppermost meter of the unsaturated zone after rainfall events; however, much of this infiltrated water is later evapotranspired. Monthly monitoring of moisture content with a neutron probe to depths of 41 m (135 ft) shows that recharge pulses are not moving deeply into the unsaturated zone. Water potentials as low as –15.6 MPa indicate that the system is very dry. Water-potential gradients generally indicate upward water movement, under isothermal conditions, except in the shallow subsurface immediately after precipitation events.

Temperature decreases with depth from April to October and increases with depth during the remainder of the year; therefore, temperature gradients oppose water potential gradients during the summer and may result in downward movement of water vapor.

Chloride Mass Balance

Chloride concentrations in soil water have been used to evaluate moisture fluxes in semi-arid systems (Bresler, 1973; Peck, 1981; Sharma, 1985; Johnston, 1987). Chloride is an ideal tracer because it is chemically conservative and, as a trace nutrient, plant uptake of chloride is minimal. Chloride concentrations increase through the root zone by evapotranspiration and remain constant below the root zone. Because chloride in soil water is concentrated by evapotranspiration, chloride concentrations are inversely proportional to water velocities. According to the theory of chloride transport (Bresler, 1973; Peck and others, 1981), the solute flux (J_s) , under steady-state conditions, can be described by

$$J_s = -D((\theta,v)) \frac{\partial c}{\partial z} + c\, q_w + S \quad , \tag{1}$$

where D is the hydrodynamic dispersion coefficient, a function of θ (the volumetric moisture content) and v (the average soil moisture velocity); z is the vertical space coordinate; c is the concentration; q_w is the volumetric soil-moisture flux; and S is a source term. Rearranging equation (1) yields the soil-moisture flux

$$q_w = \frac{1}{c}\left(J_s + D(\theta,v) \frac{\partial c}{\partial z} - S\right). \tag{2}$$

Eolian, fluvial, and lacustrine sediments generally do not contain chloride of pedogenic origin; therefore, the source term is minimal in these systems. If the hydrodynamic dispersion coefficient also is negligible, equation (2) can be simplified to

$$q_w = J_s / c, \tag{3}$$

where J_s for chloride is approximated by the mean annual precipitation rate (p) times the mean chloride concentration in precipitation and in dry fallout (Cl_p) (Sharma, 1985; Mattick, 1987). The moisture flux is divided by the volumetric moisture content to obtain the specific moisture flux (q_w/θ). The travel time (t) represented by chloride at depth z can be evaluated by dividing the total mass of chloride concentration from the surface to that depth by the chloride flux

$$t = \frac{\Sigma Cl_{sw} \times z}{P \times Cl_p}, \qquad (4)$$

where c is approximated by Cl_{sw} (mean chloride concentration in soil moisture below the root zone).

Although the chloride mass-balance theory predicts that chloride concentrations should increase through the root zone and remain constant below the root zone, most chloride profiles described in the literature show that chloride concentration decreases below the peak. This reduction in chloride has been attributed to ground-water dilution (Phillips, 1988), non-piston-type flow (Sharma, 1985), or paleoclimatic variations (Allison, 1985). Specific moisture flux estimates from chloride concentration data in semiarid regions in New Mexico range from 0.1 to 4 mm a^{-1} (0.004 to 0.16 inch a^{-1}) (Mattick, 1987). Recharge rates in South Australia varied with topographic setting and ranged from ≤0.1 mm a^{-1} (0.004 inch a^{-1}) in sand dunes to ≥100 mm a^{-1} (≥4 inches a^{-1}) in sinkholes (Allison, 1985). Approximately 50,000 yr of recharge is calculated to be stored in the thick (30 to 40 m [198 to 131 ft]) unsaturated zone of this region (Allison, 1985).

Anthropogenic Radioisotopes

The penetration depths of radioisotopes such as ^{36}Cl and ^{3}H can be used to estimate the moisture flux by dividing the peak depth by the elapsed time since peak fallout. This method assumes unidirectional steady-state flow. The ^{36}Cl isotope has a half-life of 3.01×10^5 yr. Natural ^{36}Cl is produced by cosmic ray spallation of ^{40}Ar and neutron activation of ^{36}Ar (Bentley, 1986). The ratio of natural ^{36}Cl to stable chloride ($^{36}Cl/Cl$) in the study area is approximately 0.5×10^{-12}

(Fig. 3). ^{36}Cl was enriched in the atmosphere by neutron activation of ^{35}Cl in sea water by weapons tests conducted in the South Pacific between 1952 and 1958, which peaked in 1955 (Bentley, 1986). Temporal variations in ^{36}Cl fallout were predicted on the basis of an atmospheric box model (Fig. 4). Latitudinal variation in ^{36}Cl, evaluated using ^{185}W, indicates that the total ^{36}Cl fallout in the southwestern United States was approximately 3.4×10^{12} atoms m^{-2} (Phillips, 1988). The use of ^{36}Cl data to estimate moisture flux in the unsaturated zone is relatively new and previously has been applied only at five different sampling locations, three in New Mexico and two in Nevada (Phillips, 1988; Norris, 1987). The $^{36}Cl/Cl$ peaks were observed in those studies at depths of 0.5 to 1.5 m (1.6 to 4.9 ft) and yielded specific moisture fluxes of 1.8 to 3 mm a^{-1} (0.07 to 0.12 inch a^{-1}).

Tritium has a half-life of 12.43 (± 0.05) yr and is produced naturally by the interaction of ^{14}N with cosmic-ray neutrons according to the following reaction (IAEA, 1983):

$$^{14}_{7}N + 10\ n = {}^{12}_{6}C + {}^{3}_{1}H. \qquad (5)$$

Natural production is approximately 10 tritium units (1 TU is 1 ^{3}H atom in 10^{18} atoms of ^{1}H or 0.118 becquerel (Bq) kg^{-1}). Bomb ^{3}H was produced initially in 1952, and peak production followed in 1963–1964. Tritium concentrations increased from 10 to ≥2000 TU during atmospheric nuclear testing (IAEA, 1983). Temporal variations in average ^{3}H concentrations for the Northern Hemisphere are shown in figure 4; however, ^{3}H fallout depends on local precipitation and may be highly variable. Moisture flux can be estimated from the ^{3}H peak depth and also by ^{3}H mass balance if the 1962–1965 ^{3}H peak can be identified. This latter approach uses the equation

$$q_w = ep\ (ts/ti), \qquad (6)$$

where ep is the effective precipitation (precipitation - actual evapotranspiration), ts is the total amount of post-1955 ^{3}H in the soil profile, and ti is the ^{3}H input to the soil since 1955. Specific moisture flux based on the ^{3}H peak method was approximately 9 mm a^{-1} (0.35 inch a^{-1}) in New Mexico, whereas that based on the mass-balance method was 6 mm a^{-1} (0.24 inch a^{-1}) (Phillips, 1988).

Applied Tracers

In many studies, tracers such as Cl^-, Br^-, and ^3H are applied on the land surface to evaluate unsaturated flow and solute transport. Large concentrations of these tracers generally are applied to allow easy distinction between the applied and background concentrations. Background bromide concentrations are generally negligible in soils. The above tracers are chemically conservative and are used to evaluate advective flow independent of chemical reactions. In experiments, these tracers are transported into the subsurface under constant flux or ponding conditions. Temporal variations in the tracer distribution then are determined by sampling water with soil-solution samplers or by coring soil and extracting water samples. Tracers also are used to evaluate natural infiltration by allowing precipitation to leach the tracers (Sharma, 1985). The spatial variability of infiltration rates is determined from these data. Soil-water samples collected and analyzed at different times allow unsaturated flow velocities and dispersion coefficients to be estimated. Water velocities based on the tracer data at some sites are slightly less than or equal to velocities based on water balance data (Biggar, 1976; Van De Pol, 1977; Jury, 1982), and at other sites they are from 2 to 11 times greater than water balance velocities (Bowman, 1986; Kies, 1981). The higher velocities calculated from the tracer data are attributed to bypass or preferential flow, although the soils in those experiments appeared structurally uniform.

METHODS

Field Methods

To determine ambient moisture and chloride contents from 10 boreholes drilled during July and August 1988 and in January and February 1989, approximately 230 soil samples were collected (Fig. 5). One borehole (no. 18) was drilled with a rotary rig with air as a circulation fluid,

and samples were collected with a split spoon to 22 m (72 ft). The remaining boreholes were rotary drilled with hollow-stem augers, and samples were collected at each interval in shelby tubes. No drilling fluids were used. These boreholes generally were drilled to the top of the clay-rich Fort Hancock Formation, at a depth of approximately 15 m (49 ft), which the auger could not penetrate. Boreholes 23 and 27 were further deepened with a wireline drill rig. The sampling interval varied from approximately 0.3 to 1 m (1 to 3 ft). At least 80 g of sample was collected for moisture and chloride analysis. These samples were placed in PVC sample cups, sealed with parafilm and taped to prevent moisture loss, and weighed in the field. Although volumetric moisture content could not be directly determined in 90% of the samples because the material was not sufficiently cohesive, volumetric moisture content of these samples was calculated from gravimetric moisture content using a bulk density of 1.4 (average bulk density measured in 27 samples).

In addition to samples for analyses of moisture and chloride content, 26 samples were collected for ^{36}Cl analysis in January 1989 (Fig. 5). The sampling interval was predetermined from a chloride profile in borehole 50 that suggested that water had infiltrated to a depth of 0.5 m (1.6 ft) during the last 35 yr. Five samples were collected above the predicted peak depth to define the actual peak. Samples were collected at 0.1-m (0.3-ft) intervals with a trowel from a 1-m-deep (3-ft-) pit and stored in plastic bags. The amount of soil required to obtain 20 mg of chloride was calculated from chloride concentration data (borehole 50) and ranged from 10 kg near the surface to 1 kg at depth. Core samples were collected at depths greater than 1 m (3 ft) with shelby tubes in a hollow-stem auger, as described above; samples were sealed in glass jars. Subsamples for moisture and chloride content were sealed in plastic cups.

Samples for ^{3}H analyses were collected at the same depth intervals and by the same techniques used to collect samples for ^{36}Cl. The 1-kg soil mass required to obtain approximately 0.05 l of water for ^{3}H analyses was calculated from moisture content data from nearby borehole 50. These samples were stored in plastic bags and were sealed under vacuum.

A 10 × 10 m (33 × 33 ft) test plot was irrigated with approximately 30 mm (1.2 inches) of $Ca(Br)_2$ solution (concentration: 2,200 g m^{-3}) in October 1988. The natural vegetation was grass.

The irrigation system consisted of 31 parallel lines of drip tubing (Iridelco Co., Fresno, CA) spaced 0.3 m apart. The tubing contained 16 mm in line emitters at 0.3-m (1-ft) intervals. The emitters in adjacent lines were offset by 0.15 m (0.5 ft) to allow more uniform tracer application. Drip uniformity tests conducted on a similar irrigation system showed that the water application from these systems is highly uniform (Wierenga, 1988). The tracer was pumped from a 4 m^3 (14 ft^3) tank through the irrigation system for 2 hr. The area was subsequently leached by natural precipitation events. Soil samples were collected at approximately 30-mm intervals from three profiles to depths of 0.4 m (1.3 ft) and were analyzed for moisture content and bromide concentration.

Laboratory Methods

Gravimetric moisture content was determined by drying at least 80 g of soil at 105°C for two 24 hr periods. The incremental weight loss during the period was less than 5% of the original weight loss. To determine chloride content, double-deionized water was added to the dried soil sample in a 1:1 or 2:1 ratio. Samples were agitated on a reciprocal shaker table for 8 hr, then centrifuged for 10 min at 5,000 rpm. The supernatant was filtered through 0.45 μm filters. Chloride was then analyzed by ion chromatography or by potentiometric titration; bromide was analyzed by ion chromatography. To test if oven drying had any effect on chloride concentration, four samples were split and one half of each was oven dried. Comparison of the chloride concentrations of the splits showed that oven drying had no effect on chloride concentrations. Water fluxes were calculated for each depth interval from the chloride concentration data according to equation 3. The mean chloride concentration Cl_p (0.29 g m^{-3}), which includes chloride in precipitation and in dry fallout, was calculated from the pre-bomb $^{36}Cl/Cl$ ratio (0.46×10^{-12}) measured in soil water from borehole 51, and the natural ^{36}Cl fallout at the site estimated as 20 atoms ^{36}Cl m^{-2} s^{-1} (Bentley and others, 1986).

Textures of approximately 100 soil samples were measured. The samples were ground to disaggregate calichified materials. The greater-than-2-mm (>0.08-inch) fraction was determined by dry sieving, and the percent sand, silt, and clay was evaluated by hydrometer analysis following Bouyoucos (1962).

The $^{36}Cl/Cl$ ratios were measured by Tandem Accelerator Mass Spectrometry (TAMS) at the University of Rochester, Rochester, New York (Elmore, 1979). Laboratory preparation of ^{36}Cl samples for analysis followed procedures outlined in Mattick and others (1987). Double-deionized water was added, and the mixture was stirred with an electric stirrer for approximately 12 hr. AgCl was precipitated from the chloride solution by addition of $AgNO_3$. Because ^{36}S interferes with ^{36}Cl analysis, $Ba(NO_3)_2$ was added to the solution to precipitate $BaSO_4$. Isotopic ratios of one split of the samples from the top meter were diluted in a 1:1 ratio with chloride because $^{36}Cl/Cl$ ratios of less than 5×10^{-12} are preferred for analysis and because measured peak ratios of bomb $^{36}Cl/Cl$ are up to 20×10^{-12} in some areas (Phillips, 1988). The chloride consisted of Weeks Island halite from Louisiana, which contains no ^{36}Cl. In order to evaluate chemical contamination during sample preparation, the chloride blank was subjected to the same purification procedure as the soil samples. The AgCl samples were wrapped in aluminum foil to prevent reduction of Ag^+ to Ag prior to analysis.

Because TAMS measurements take approximately 1 to 2 hr per sample, the 10 uppermost samples that had been diluted with chloride were initially scanned to determine the approximate position of the bomb peak and to evaluate ^{36}S interference. All $^{36}Cl/Cl$ ratios were less than 5×10^{-12}. In 5 of the 10 samples scanned, ^{36}S contamination had occurred, possibly related to the use of latex gloves during sample loading; therefore, new uncontaminated samples were reloaded before final analysis. Each run consisted of four samples, two standards that had a $^{36}Cl/Cl$ ratio of 1.6×10^{-12}, and a blank. A total of 12 samples and a blank were run. The $^{36}Cl/Cl$ ratios from the Weeks Island halite blank were similar to those of the University of Rochester blank and indicated that no chemical contamination had occurred during sample processing. Uncertainties were calculated according to Elmore and others (1984) and are reported as one standard deviation.

Water for ^{3}H analyses was extracted from soil samples by azeotropic distillation with toluene. The soil samples were covered with toluene and subsequently heated to 100 °C. After distillation the water samples were purified of toluene by heating in paraffin wax. The water was sealed in glass bottles that had been purged with argon gas. Tritium was determined by direct liquid scintillation at the University of Waterloo, Ontario, Canada. Analytical precision of the ^{3}H analyses is ± 8 TU.

RESULTS

Soil Texture and Moisture Content

The average sand percent in the shallow (12 to 15 m [39 to 49 ft]) material (Camp Rice Formation) ranges from 50 to 60%, whereas clay and silt average 10 to 20% each (Figs. 6 and 7, Table 1). Some shallow zones contain up to 60% gravel. Sediment samples that contained gravel were classified according to Folk (1974) and those that did not contain gravel were classified according to the U.S. Department of Agriculture (1975). The predominant textural types in the shallow material are sandy-clay loam to sandy loam (Table 1).

The moisture contents of the upper 0.5 m (1.6 ft) of boreholes 15 and 50 were as great as 26% following precipitation events (Fig. 6b and 6f). Below this shallow zone, low moisture contents are characteristic of coarse-grained material, whereas high moisture contents typify clay-rich sediments. This relationship is most apparent in borehole 74, where a marked increase in moisture content (≤ 0.3 m^3 m^{-3} [≤ 0.3 ft^3/ft^3]) at a depth of 8.5 m (25.5 ft) corresponds to the contact between shallow, generally coarser-grained material (Camp Rice Formation) and deeper clays (Fort Hancock Formation) (Fig. 6i and 6j, Table 1). A similar relationship exists between moisture content and grain size within the shallow coarser material, although grain-size variation among samples is less. There is no systematic difference between moisture content of samples from stream versus interstream settings (Figs. 6 and 7).

Chloride Mass Balance, ^{36}Cl, ^{3}H, and Bromide

The chloride profiles are characterized by low chloride concentrations at depths of generally less than 0.3 m (Figs. 8 and 9, Tables 2 and 3). Maximum chloride concentrations range from 1,900 to 9,300 g m^{-3}, and the depth of the maximum concentrations ranges from 1.3 to 4.6 m (4 to 15 ft). With the exception of chloride data from boreholes 21, 23, and 31, chloride peaks are relatively sharp and the profiles are smooth. Similar chloride concentrations were recorded in closely spaced boreholes (50 and 51, 10 m apart; Table 2). There is no systematic relationship between geomorphic setting and maximum chloride concentration data (Table 3).

Contrary to the chloride mass-balance theory, which predicts that chloride concentrations should increase with depth through the root zone and remain constant below the root zone, all chloride profiles in the Hueco Bolson showed a decrease in chloride concentration below the peak (Figs. 8 and 9, Table 2); therefore, estimation of moisture fluxes using this model is difficult. Specific moisture fluxes calculated according to equation 3 from chloride concentrations for each depth interval ranged from 0.2 to 7 mm a^{-1} (0.008 to 0.28 inch a^{-1}) and were ≤3% of the long-term mean annual precipitation rate (Table 2). Higher moisture fluxes (≤25 mm a^{-1}) in the upper 2 m (6.6 ft) of the unsaturated zone, which composes the root zone, were excluded in this estimate because much of this water is expected to be evapotranspirated. Because the chloride profiles do not conform to the chloride mass-balance theory, these calculated moisture fluxes are suspect.

The $^{36}Cl/Cl$ profile includes a well-defined peak of 6.6×10^{-12} at 0.5 m (1.6 ft) depth (Fig. 10, Table 4). A background ratio of 0.46×10^{-12} below 1.25 m (4.1 ft) agrees with the predicted natural fallout of 0.5×10^{-12} for this latitude (Bentley and others, 1986) (Fig. 3). The total inventory of bomb ^{36}Cl is 2.5×10^{12} atoms m^{-2} in borehole 51, which is 73% of the predicted fallout at this latitude (3.4×10^{12} atoms m^{-2} [Phillips, 1988]). The maximum $^{36}Cl/Cl$ ratio indicates that the specific moisture flux to 0.5 m (1.6 ft) depth during the past 35 yr is 1.4 mm a^{-1} (0.06 inch a^{-1}), or 0.5% of the mean annual precipitation rate in the region. The specific

flux calculated from the total penetration of bomb ^{36}Cl (~1 m [~ 3ft] depth) is 3.5 mm a^{-1} (0.14 inch a^{-1}).

The ^{3}H profile consists of three peaks that are of approximately equal magnitude (23 to 29 TU) (Fig. 10, Table 4). If piston-type flow is assumed, the surface peak should represent the most recent precipitation, whereas the deepest peak should represent the 1963–1964 bomb pulse. Although the 1963–1964 peak would be expected to be greater than the other peaks based on the ^{3}H fallout, sample contamination appears unlikely because samples from the same depth intervals in a nearby borehole yielded similar results. A specific moisture flux of 7 mm a^{-1} (0.28 inch a^{-1}) was calculated by assuming that the peak at 1.4 m (4.6 ft) depth represents 1963–1964 recharge. Specific moisture fluxes were not calculated with the ^{3}H mass-balance approach because effective precipitation estimates are grossly inaccurate. At 0.9 to 1 m (3.0 to 3.3 ft) depth, ^{3}H concentrations were below the detection limit. At a specific moisture flux of 7 mm a^{-1} (0.28 inch a^{-1}), this ^{3}H low corresponds to water flux between 1971 and 1973.

The artificially applied bromide penetrated to a maximum depth of approximately 0.3 m (1 ft) after 1 yr (Fig. 11a). Because bromide was initially applied with 3 mm (0.12 inch) of irrigation water, the penetration depth of bromide that resulted from subsequent precipitation events is less than that recorded in these profiles. The maximum bromide concentration in the soil water was recorded at depths that ranged from 0.11 to 0.18 m (0.36 to 0.59 ft). The bromide was applied at a concentration of 2,200 g m^{-3} and the maximum observed concentration in the soil water ranged from 4,300 to 6,300 g m^{-3},which indicates that bromide was concentrated in the soil profile by evapotranspiration. Because the initial application of the tracer was assumed to be uniform, the difference in the shape and peak depths of bromide among the profiles is attributed to spatial variability in natural soil moisture flux. The recovery of bromide ranged from 90 to 130% in the profiles, and the variation in recovery is attributed to inaccuracies in the estimation procedure. Moisture content was similar in all three profiles and increased from 0.04 to 0.1 m^3 m^{-3} (0.04 to 0.1 ft^3/ft^3) at 0.15 m depth and remained relatively constant below this depth (Fig. 11b).

DISCUSSION

Variations in soil moisture are related to both climatic and grain-size controls. High moisture contents recorded in the uppermost 0.5 m (1.6 ft) of the unsaturated zone were recorded only following precipitation events. At greater depths, soil moisture content is controlled primarily by variations in sediment grain size: coarse-grained material has low moisture content and clay-rich sediment has high moisture content.

Chloride profiles provide only a qualitative estimate of average recharge rates because the many assumptions associated with this model are not all ideally satisfied: (1) chloride concentration increases with depth below land surface because of evapotranspiration, then remains constant with depth below this peak value; (2) one-dimensional, vertical, piston-type flow applies; (3) precipitation is the only source of chloride; (4) mean annual precipitation and chloride concentration of precipitation remain constant through time; and (5) subsurface flow conditions are at steady state (Sharma, 1985). Like most chloride profiles described in the literature, chloride profiles in the Hueco Bolson show a decrease in chloride concentration with depth below the peak, which suggests that some assumptions associated with the chloride mass balance approach may not be valid. In an arid region of New Mexico, proximal to a discharge zone where the water table is shallow (approximately 5 m [16.4 ft]), a reduction in chloride concentration below the root zone was attributed to dilution with ground water in areas of shallow water tables (Mattick, 1987). The water table below the Hueco Bolson, however, is deep (≥130 m). The assumption of one-dimensional vertical flow in the Hueco Bolson is reasonable, and no significant lateral flow in the unsaturated zone is expected because all boreholes except 74 were drilled in topographically flat areas with slopes of less than 1%. Although non-piston-type flow has been used to explain the decrease in chloride concentrations in some profiles (Sharma, 1985), it is difficult to test whether piston-type flow occurs. The existence of a single ^{36}Cl peak in the Hueco Bolson, rather than the multiple peaks that were recorded in other regions (Phillips, 1988; Norris, 1987), suggests that

piston-type flow is likely. Because the sediments in the Hueco Bolson are terrestrial in origin, it is unlikely that chloride in the unsaturated zone has a source other than precipitation. The decrease in soil water chloride concentration below the peak may represent temporally varying precipitation, chloride input, moisture flux, or other environmental conditions (Allison, 1985). Decreases in chloride concentrations in profiles in South Australia were explained by a greater moisture flux in the past that corresponded to paleoclimatic variations. Paleoclimatic data for the southwestern United States suggest that the climate was wet during the Pleistocene and became progressively drier during the past 8,000 yr (Baumgardner, 1990).

To examine the possibility of changing environmental conditions, cumulative chloride concentration was plotted against cumulative water content for each borehole (Figs. 8 and 9). Cumulative water content was used instead of depth to factor out variations in water content (Allison, 1985). Moisture fluxes were calculated from the straight-line portions of these plots, which signify uniform environmental conditions. In these flux calculations, Cl_{sw} is the weighted mean soil water chloride concentration in a depth interval with a constant gradient in cumulative-chloride-versus-water-content that indicates uniform environmental conditions. Most profiles have multiple line segments or curved lines that indicate varying environmental conditions. Some profiles (23, 31; Fig. 9e and 9n) have a single straight segment, which indicates uniform conditions for the time period recorded by the borehole samples. Specific moisture fluxes for the latter profiles ranged from 0.04 to 0.05 mm a^{-1} (0.0016 to 0.0020 inch a^{-1}). Those profiles that record varying conditions with time are characterized by steeper cumulative-chloride-versus-water-content profiles with depth, which reflect past conditions with greater water and/or chloride flux than present rates of flux. A gradual steepening of the cumulative-chloride-versus-water-content on most plots makes precise delineation of periods of change arbitrary. If a constant chloride flux is assumed, calculated recharge rates range from 0.03 to 0.7 mm a^{-1} (0.001 to 0.03 inch a^{-1}). Many of the profiles indicate that recharge rates decreased from approximately 7,000 yr to present, which is consistent with paleoclimatic data (Baumgardner, 1990).

Comparison of chloride age data and $^{36}Cl/Cl$ data analyzed in the same soil samples from borehole 51 shows that the ionic chloride data underpredict the position of the isotopic chloride peak by 0.2 m (0.6 ft) (Fig. 12). In contrast, the predicted depth of the $^{36}Cl/Cl$ bomb peak based on the chloride mass balance age data from borehole 50 agrees well with the actual $^{36}Cl/Cl$ peak depth. The specific moisture flux calculated from the $^{36}Cl/Cl$ peak (1.4 mm a^{-1} [0.055 inch a^{-1}]) is similar to that based on chloride mass balance (1.6 mm a^{-1} [0.063 inch a^{-1}]) for the same depth interval in borehole 51 (Table 2). Ionic chloride age data underpredict the depth of the ^{3}H peak because the specific moisture flux based on ^{3}H is greater than that based on chloride (Fig. 13). The specific moisture flux calculated from the ^{3}H data is also much higher than that from the $^{36}Cl/Cl$ peak (Fig. 10) because ^{3}H penetrates deeper than ^{36}Cl, although peak ^{3}H fallout occurred later than that of ^{36}Cl (Fig. 4).

Comparison of Physical and Chemical Approaches

Results of soil-physics monitoring (Scanlon and others, 1990) were compared with chemical tracer data to evaluate controls on flow in the unsaturated zone. Because the physical data indicate a potential for upward water movement under isothermal conditions, the ^{36}Cl concentration data were compared to distributions predicted by equations for ionic diffusion or advective-dispersive transport to determine if these processes could account for the distribution of ^{36}Cl in the soil profile. The one-dimensional diffusion equation to be solved is

$$D_e \frac{\partial 2c}{\partial z^2} = \frac{\partial c}{\partial t}, \qquad (7)$$

where D_e is the effective diffusion coefficient and t is time. As an initial condition, ^{36}Cl was assumed to be uniformly distributed in the upper 0.2 m (0.6 ft) of the soil zone. This depth represents the maximum penetration depth of the wetting fronts observed during the monitoring period. D_e was estimated to be 1.4×10^{-3} m^2 a^{-1} on the basis of laboratory data for silty clay loam

at 13% moisture content (Porter, 1960). The following Laplace solution of the diffusion equation (Carslaw, 1959) was used to solve for ^{36}Cl concentrations for an infinite soil column:

$$c = 0.5\, c_o \left\{ \operatorname{erf} \frac{a-z}{2\sqrt{D_e \times t}} + \operatorname{erf} \frac{a+z}{2\sqrt{D_e \times t}} \right\}, \quad (8)$$

where C_o is the initial concentration of 12.4×10^{12} atoms $^{36}Cl\ m^{-3}$ in the upper 0.2 m (0.6 ft) (a) and the time was 35 yr. Comparison of the calculated and observed ^{36}Cl concentration profiles indicates that diffusion alone cannot account for the observed ^{36}Cl profile (Fig. 14) and that advective flow must also be included.

An analytical solution of the one-dimensional advective-dispersive equation (van Genuchten, 1982) was used as a model of the ^{36}Cl profile:

$$\frac{\partial c}{\partial t} = D \frac{\partial^2 c}{\partial z^2} - v \frac{\partial c}{\partial z}, \quad (9)$$

where D is the hydrodynamic dispersion coefficient and v is the pore-water velocity. Although flow in the shallow unsaturated zone is much more complex than suggested by this equation, which assumes unidirectional water movement with uniform velocity, more complex models were not used because detailed information for the past 35 yr on spatial and temporal variations in flow directions and velocities required for their solution were not available. A uniform downward seepage velocity of 22 mm a^{-1} (0.87 inch a^{-1}) was used on the basis of the depth of the peak ^{36}Cl concentration. The computer program of the analytical solution was modified to allow pulsed input of the ^{36}Cl concentrations with a step function (Fig. 15). Only 73% of the predicted bomb fallout ratio was recovered at the site; therefore, the fallout was reduced by this amount as input for the model. The $^{36}Cl/Cl$ fallout ratio was converted to ^{36}Cl concentrations and was approximated with a step function (Fig. 15). An initial estimate of the hydrodynamic dispersion coefficient was modified to obtain the best fit between the predicted and the observed ^{36}Cl concentrations. The hydrodynamic dispersion coefficient indicates the degree of mechanical mixing and molecular diffusion in the system; a large hydrodynamic dispersion coefficient results in a broad, low peak,

whereas a low hydrodynamic dispersion coefficient yields a narrow, high peak. Good agreement between simulated and observed ^{36}Cl concentrations was obtained when a dispersion coefficient of 1.0×10^{-3} m^2 a^{-1} was used (Fig. 16). This hydrodynamic dispersion coefficient is similar to the previously estimated diffusion coefficient of 1.4×10^{-3} m^2 a^{-1}. Because the hydrodynamic dispersion coefficient includes the effects of both mechanical mixing and molecular diffusion, this calculated dispersion coefficient is unrealistically low (i.e., the ^{36}Cl peak is unrealistically narrow and high). The low dispersion coefficient suggests that the ^{36}Cl peak possibly was intensified by repeated alternation of the flux vector from downward (infiltration) to upward (evapotranspiration) and indicates that the distribution of ^{36}Cl cannot be simulated with unidirectional water movement.

Bromide, ^{3}H, and ^{36}Cl profiles indicate a net downward flux opposite to the upward-directed water-potential gradients. Movement of chloride and bromide is restricted to liquid-phase flow because these ions are nonvolatile. The discrepancy between specific moisture fluxes based on ^{36}Cl and ^{3}H data from Hueco Bolson is similar to that from New Mexico, where the discrepancy was attributed to ^{3}H transport in the vapor phase and the vapor transport hypothesis was supported by experimental data (Phillips, 1988). Water potentials as low as -16 MPa near the surface in Hueco Bolson indicate that the unsaturated zone is extremely dry and that much of the water is probably in the vapor phase. Although temperature gradients are reversed in the winter at shallow depths (0.5 m [1.6 ft]), the greater downward-directed temperature gradients in the summer as a result of solar radiation and the higher temperatures during this period (Scanlon, 1990) should produce larger vapor pressure gradients that could account for the net downward movement of ^{3}H in the vapor phase.

Radioisotopic tracer data indicate that flow processes in the shallow unsaturated zone are complex, with repeated cycles of infiltration and evapotranspiration and with long-term (30 yr) net movement of water directed downward. Comparison of ^{3}H and ^{36}Cl data suggests that temperature gradients are also important in the shallow zone. These anthropogenic tracers have moved to depths of less than 2 m (6.6 ft); therefore, the magnitude of the moisture flux in deeper sections of the unsaturated zone cannot be estimated from these tracers. Results of the chloride mass balance

and ^{36}Cl methods agree for the top 2 m (6.6 ft) and suggest that the downward movement of water should continue at least through the uppermost 20 m (66 ft) of the unsaturated zone.

It is difficult to compare the results of physical studies with chloride mass-balance data because of the many assumptions associated with the latter. If water movement was predominantly upward, as indicated by the water potential gradients, the highest chloride concentrations should occur at the surface; however, maximum chloride concentrations were observed at 2 to 5 m (6.6 to 16 ft) depth. The discrepancy between the chloride and soil physics data is not fully resolved because of the lack of other suitable tracers at depths greater than 2 m (6.6 ft) in the unsaturated zone.

Comparison of Hueco Bolson Chemical Tracer Data with Data from Other Regions

Results of tracer studies conducted at Hueco Bolson were compared with those from other regions to better understand the environmental controls on water flow in arid regions. Three sites in central New Mexico (NMSUR, SNWR1, and SNWR2, Table 5) were compared (Phillips and others, 1988). Comparisons of fluxes from the Hueco Bolson and the sites in New Mexico are most valid because climatic conditions in both regions are similar (Table 5). The total inventory of ^{36}Cl at the Hueco Bolson is similar to that measured at NMSUR but is approximately three times higher than that recorded at the SNWR sites in New Mexico. These differences in total inventories may represent local variations in ^{36}Cl fallout. Specific moisture flux based on the ^{36}Cl data from Hueco Bolson is most comparable with that from the SNWR2 site in New Mexico; multiple ^{36}Cl peaks recorded at the other two sites in New Mexico make comparisons difficult. The $^{36}Cl/Cl$ peak was 0.4 m deeper at SNWR2 than at Hueco Bolson, and the resultant specific moisture flux at SNWR2 was approximately twice that at Hueco Bolson (Fig. 17; Table 5). Although the ^{36}Cl-based specific moisture flux for the Yucca Wash site in Nevada (1.8 mm a^{-1} [0.07 inch a^{-1}]) is similar to that recorded at Hueco Bolson, the mean annual precipitation at the Nevada site is approximately half that recorded at Hueco Bolson. The percentage of mean annual precipitation that

infiltrates was calculated by dividing the mean annual precipitation by the specific moisture flux and is much higher in New Mexico (1.1 to 1.5%) and in Nevada (1.2%) than in Hueco Bolson (0.5%) and may result from coarser-grained materials at the other sites (Table 5).

In all the New Mexico sites and in Hueco Bolson, ^{3}H profiles consisted of three peaks (Phillips, 1988). The ^{3}H concentrations of the 1963–1964 peaks, however, were much greater in New Mexico (60 to 90 TU) than in Hueco Bolson (28 TU). Compared with the below-normal precipitation at Hueco Bolson during the period of peak fallout (1963–1965), the normal precipitation in New Mexico may account for the discrepancy in peak concentrations. A ^{3}H low that was estimated to occur in the 1972–1973 period was recorded at all New Mexico sites and at Hueco Bolson. Downward movement of ^{3}H at NMSUR (1.4 m [4.6 ft]) and in Hueco Bolson (1.4 m [4.6 ft]) was less than that at SNWR1 (2.5 m [8.2 ft]), which is attributed to the predominance of coarser material at SNWR1 (Phillips, 1988) (Table 5). Although the penetration depths of ^{3}H vary, the specific moisture fluxes of all three sites are similar (6 to 8.4 mm a^{-1} [0.2 to 0.3 inch a^{-1}]) because of lower moisture contents in the coarser-grained material. The ^{3}H data also indicate that the percentage of precipitation that infiltrates in New Mexico is approximately twice that in Hueco Bolson. The high percentage of precipitation (≤30%) that infiltrates in the Dahna sand dunes of Saudi Arabia is attributed to the coarse grain size of the sand dune sediments and to steep temperature gradients that result in downward vapor movement (Dincer, 1974).

Specific moisture fluxes based on chloride and tritium data agree well in humid regions such as South Australia and Cyprus (Allison, 1978; Kitching, 1980). In arid regions, such as parts of New Mexico and Texas, the specific moisture fluxes based on ^{3}H data are much higher than those based on ^{36}Cl and chloride data. The faster transport of tritium relative to chloride or ^{36}Cl in arid regions is attributed to ^{3}H transport in the vapor phase (Phillips, 1988), whereas vapor transport is negligible in humid regions.

Comparisons among physical and chemical data from many of these sites are difficult because information on physical attributes of these regions is limited. Physical attributes of the

three New Mexico sites differ markedly. The water table is approximately 5 m (16 ft) deep at SNWR1 and measured water potentials are high (≥ -0.1 MPa), and the calculated specific moisture fluxes based on Darcy's Law range from 7 to 37 mm a^{-1} (0.28 to 1.46 inches a^{-1}). In contrast, the water table is approximately 100 m (328 ft) deep at the other two sites in New Mexico, and measured water potentials range from -1 MPa at the surface to -5 MPa at 5 m (16 ft) depth at NMSUR (D. B. Hudson, pers. comm., 1989). Despite the large difference in physical attributes at these sites, results of chemical tracer data are remarkably similar (Table 5). The water potentials are approximately an order of magnitude lower at Hueco Bolson than at NMSUR, which indicates that the former system is much drier. Based on a comparison of the physical data, specific moisture fluxes also would be expected to be much lower in Hueco Bolson than in New Mexico. Specific moisture fluxes based on ^{36}Cl data in Hueco Bolson are approximately half those measured in New Mexico, whereas those based on ^{3}H data are similar in the two regions. The lack of general correspondence between the physical and chemical data within each study area is attributed to the complexity of flow in shallow unsaturated zones in arid regions.

Implications to Site Assessment for Low-Level Radioactive Waste Disposal

Because physical flow processes are extremely complex in the shallow unsaturated zone in arid regions, with alternating upward and downward flow of liquid and vapor phases, chemical tracer data may be more reliable than soil physical data for predicting radionuclide transport. The advantage of chemical tracers is that they record the net moisture flux over much longer time periods than are considered by soil physics monitoring. ^{36}Cl is nonvolatile and chemically nonreactive and therefore provides an upper limit to the transport rate of nonvolatile radionuclides. The migration of volatile radioisotopes, such as those of C and H, should be more closely approximated with ^{3}H tracer than with ^{36}Cl data. The degree to which chemical tracer data can be used to approximate the rate of water infiltration into the disposal facility will depend on the textural similarity between the sedimentary materials that make up the repository cover and native

sediments. The fate of radionuclides leached from the base of the facility is difficult to evaluate from tracer data because installation of the facility will markedly alter the natural system. Potential leakage from a repository is more readily assessed through numerical modeling of physical flow than through chemical tracer data. Therefore, both chemical and physical data are required to fully characterize a system for radioactive waste disposal.

CONCLUSIONS

1. Recharge rates based on the chloride mass balance approach ranged from 0.01 to 1 mm a^{-1} and were not related to geomorphic setting.
2. The $^{36}Cl/Cl$ peak was measured at a depth of 0.5 m (1.6 ft) and resulted in a specific moisture flux of 1.4 mm a^{-1} (0.06 inch a^{-1}).
3. Tritium penetrated much deeper than ^{36}Cl, and the resultant specific moisture flux was 7 mm a^{-1} (0.28 inch a^{-1}).
4. The low net downward fluxes recorded by the chemical tracers contrast with the potential upward water movement under isothermal conditions that is indicated by the water potential data. There is a lack of general correspondence between physical and chemical results from Hueco Bolson and New Mexico. In the shallow unsaturated zone, where physical flow processes are complex and have upward and downward potential gradients, chemical tracer data are more reliable in delineation of the long-term net moisture flux.
5. In arid regions including Hueco Bolson, the faster transport of ^{3}H relative to chloride or ^{36}Cl is attributed to ^{3}H movement in the vapor phase, which is controlled by downward-directed summer temperature gradients. In contrast, moisture fluxes calculated from ^{3}H and chloride data in humid regions are in good agreement because vapor transport is relatively minor.
6. The implication of this research for site assessment for radioactive waste disposal in arid regions is that chemical tracer data are more reliable than soil physics monitoring in

predicting the potential for radionuclide transport in the shallow unsaturated zone, where information on net water movement over a long time period is required. The relative importance of moisture fluxes based on ^{3}H and ^{36}Cl for radioactive waste disposal depends on the magnitude of volatile radionuclides that will be disposed of in the facility.

ACKNOWLEDGMENTS

This research was funded by the Texas Low-Level Radioactive Waste Disposal Authority under contract no. IAC(90-91)0268. The conclusions of the authors are not necessarily approved or endorsed by the Authority. We thank the drillers, J. Doss and D. Ortuno, and the chemical analyst, S. Tweedy. The assistance of W. F. Mullican III in organizing the drilling is gratefully appreciated. The ^{36}Cl analyses were conducted at the University of Rochester by P. W. Kubik and P. Sharma. A. R. Dutton provided helpful review of the report. The manuscript was edited by T. F. Hentz and A. R. Masterson. Word processing was by M. Snell. Figures were drafted by J. Jobst under the direction of R. L. Dillon.

REFERENCES

Allison, G. B., and Hughes, M. W., 1978, The use of environmental chloride and tritium to estimate total recharge to an unconfined aquifer: Australian Journal of Soil Research, v. 16, p. 181–195.

Allison, G. B., Stone, W. J., and Hughes, M. W., 1985, Recharge in karst and dune elements of a semi-arid landscape as indicated by natural isotopes and chloride: Journal of Hydrology, v. 76, p. 1–25.

Baumgardner, R. W., Jr., 1990, Geomorphology of the Hueco Bolson in the vicinity of the proposed low-level radioactive waste disposal site, Hudspeth County, Texas: The University

of Texas at Austin, Bureau of Economic Geology, contract report prepared for the Texas Low-Level Radioactive Waste Disposal Authority under contract no. IAC(90-91)0268, 98 p.

Bentley, H. W., Phillips, F. M., and Davis, S. N., 1986, 36Cl in the terrestrial environment, *in* Fritz, P., and Fontes, J.-C. (eds.), Handbook of environmental isotope geochemistry: New York, Elsevier Science, p. 422–475.

Biggar, J. W., and Nielsen, D. R., 1976, Spatial variability of the leaching characteristics of a field soil: Water Resources Research, v. 12, p. 78–84.

Bouyoucos, G. J., 1962, Hydrometer method improved for making particle size analyses of soils: Agronomy Journal, v. 54, p. 464–465.

Bowman, R. S., and Rice, R. C., 1986, Transport of conservative tracers in the field under intermittent flood irrigation: Water Resources Research, v. 22, p. 1531–1536.

Bresler, E., 1973, Simultaneous transport of solutes and water under transient unsaturated flow conditions: Water Resources Research, v. 9, p. 975–986.

Carslaw, H. S., and Jaeger, J. C., 1959, Conduction of heat in solids: London, Oxford at the Clarendon Press, 510 p.

Dincer, T., Al-Mugrin, A., and Zimmermann, U., 1974, Study of the infiltration and recharge through the sand dunes in arid zones with special reference to stable isotopes and thermonuclear tritium: Journal of Hydrology, v. 23, p. 79–109.

Elmore, D., Fulton, B. R., Clover, M. R., Marsden, J. R., Gove, H. E., Naylor, H., Purser, K. H., Kilius, L. R., Beukens, R. P., and Litherland, A. E., 1979, Analysis of 36Cl in environmental water samples using an electrostatic accelerator: Nature, v. 227, p. 22–25.

Folk, R. L., 1974, Petrology of sedimentary rocks: Austin, Texas, Hemphill, 182 p.

Gustavson, T. C., 1990, Sedimentary facies, depositional environments, and paleosols of the Upper Tertiary Fort Hancock Formation and the Tertiary-Quaternary Camp Rice Formation, Hueco Bolson, West Texas: The University of Texas at Austin, Bureau of Economic Geology, contract report prepared for the Texas Low-Level Radioactive Waste Disposal Authority under contract no. IAC(90-91)0268, 94 p.

International Atomic Energy Agency (IAEA), 1983, Isotope techniques in the hydrological assessment of potential sites for the disposal of high-level radioactive wastes: Vienna, IAEA Technical Report Series 228, chapter 7.

Johnston, C. D., 1987, Distribution of enviromental chloride in relation to subsurface hydrology: Journal of Hydrology, v. 94, p. 67–88.

Jury, W. A., Stolzy, L. H., and Shouse, P., 1982, A field test of the transfer function model for predicting solute transport: Water Resources Research, v. 18, p. 369–375.

Kies, B., 1981, Solute transport in unsaturated field soil and in ground-water, New Mexico State University, Ph. D. dissertation, 353 p.

Kitching, R., Edmunds, W. M., Shearer, T. R., Walton, N. R. G., and Jacovides, J., 1980, Assessment of recharge to aquifers: Hydrological Sciences/Bulletin des Sciences Hydrologiques, v. 25, p. 217–235.

Larkin, T. J., and Bomar, G. W., 1983, Climatic atlas of Texas: Austin, Texas Department of Water Resources Publication LP-192, 151 p.

Mattick, J. L., Duval, T. A., and Phillips, F. M., 1987, Quantification of groundwater recharge rates in New Mexico using bomb 36Cl, bomb 3H and chloride as soil-water tracers: Las Cruces, New Mexico Water Resources Research Institute, Report No. 220, 184 p.

Norris, A. E., Wolfsberg, K., Gifford, S. K., Bentley, H. W., and Elmore, D., 1987, Infiltration at Yucca Mountain, Nevada, traced by 36Cl: Nuclear Instruments and Methods in Physics Research, v. B29, p. 376–379.

Peck, A. J., Johnston, C. D., and Williamson, D. R., 1981, Analyses of solute distributions in deeply weathered soils: Agricultural Water Management, v. 4, p. 83–102.

Phillips, F. M., Mattick, J. L., and Duval, T. A., 1988, Chlorine 36 and tritium from nuclear weapons fallout as tracers for long-term liquid movement in desert soils: Water Resources Research, v. 24, p. 1877–1891.

Porter, L. K., Kemper, W. D., Jackson, R. D., and Stewart, B. A., 1960, Chloride diffusion in soils as influenced by moisture content: Soil Science Society of America Proceedings, v. 24, p. 460–463.

Scanlon, B. R., Richter, B. C., and Wang, F. P., 1990, Analysis of unsaturated flow based on physical data related to low-level radioactive waste disposal, Chihuahuan Desert, Texas: The University of Texas at Austin, Bureau of Economic Geology, contract report prepared for the Texas Low-Level Radioactive Waste Disposal Authority under contract no. IAC(90-91)0268.

Sharma, M. L., Cresswell, I. D., and Watson, J. D., 1985, Estimates of natural groundwater recharge from the depth distribution of an applied tracer: subsurface flow, pollutant transport, and salinity: Melbourne, Victoria, Australia, The Institute of Engineers, Australia National Conference Publication No. 85/13, p. 64–70.

Sharma, M. L., and Hughes, M. W., 1985, Groundwater recharge estimation using chloride, deuterium and oxygen-18 profiles in the deep coastal sands of western Australia: Journal of Hydrology, v. 81, p. 93–109.

Van de Pol, R. M., Wierenga, P. J., and Nielsen, D. R., 1977, Solute movement in a field soil: Soil Science Society of America Journal, v. 41, p. 10–13.

van Genuchten, M. J., and Alves, W. J., 1982, Analytical solutions of the one-dimensional advection-dispersion solute transport equation: U.S. Department of Agriculture, Technical Bulletin, Report No. 1661, 149 p.

Wierenga, P. J., Bachelet, D., Bilskie, J. R., Elabd, H., Hudson, D. B., Nash, M., Porro, I., Strong, W. R., Toorma, A., and Vinson, J., 1988, Validation of stochastic flow and transport models for unsaturated soils: Las Cruces, New Mexico State University, Department of Agronomy and Horticulture, Report No. 88–SS–03, 224 p.

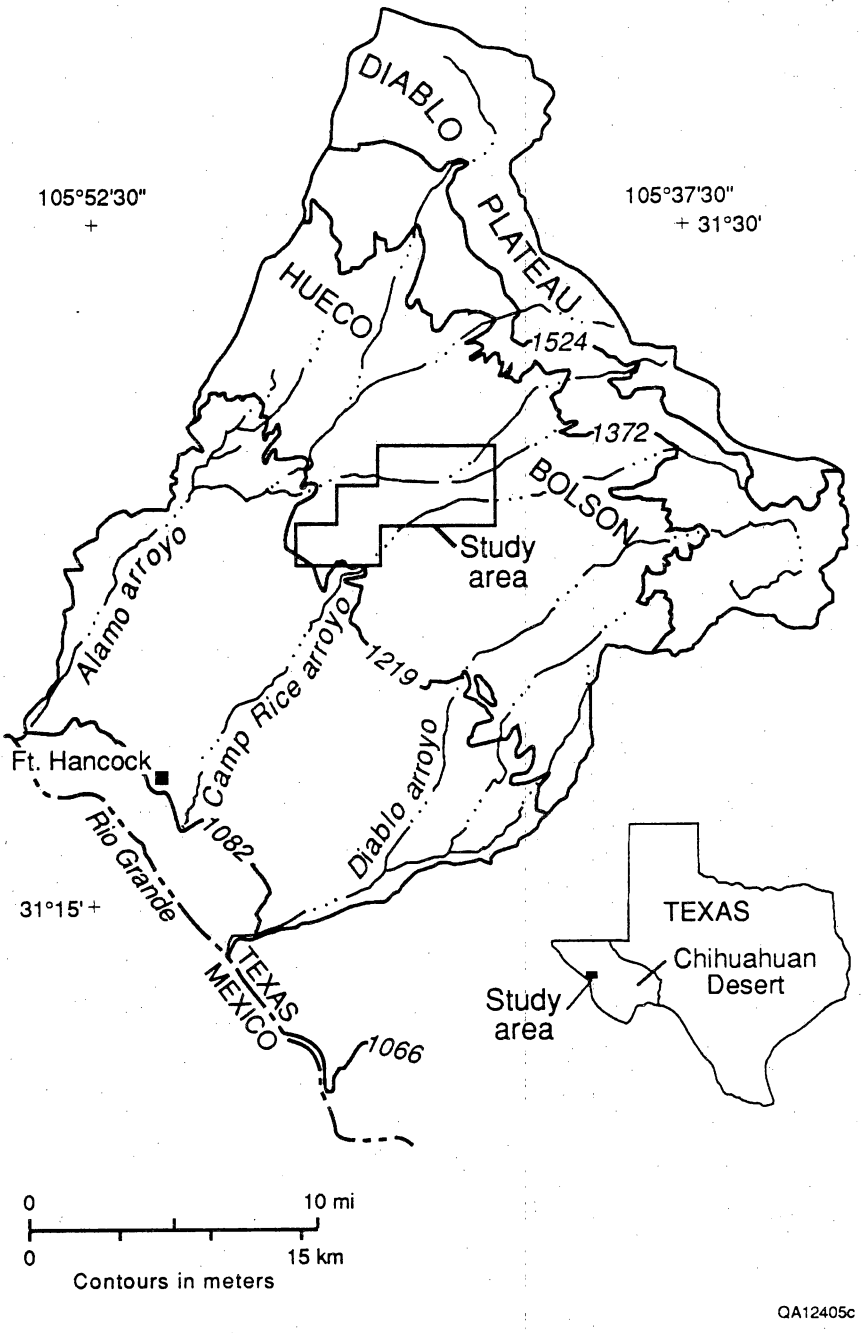

Figure 1. Location of the study area.

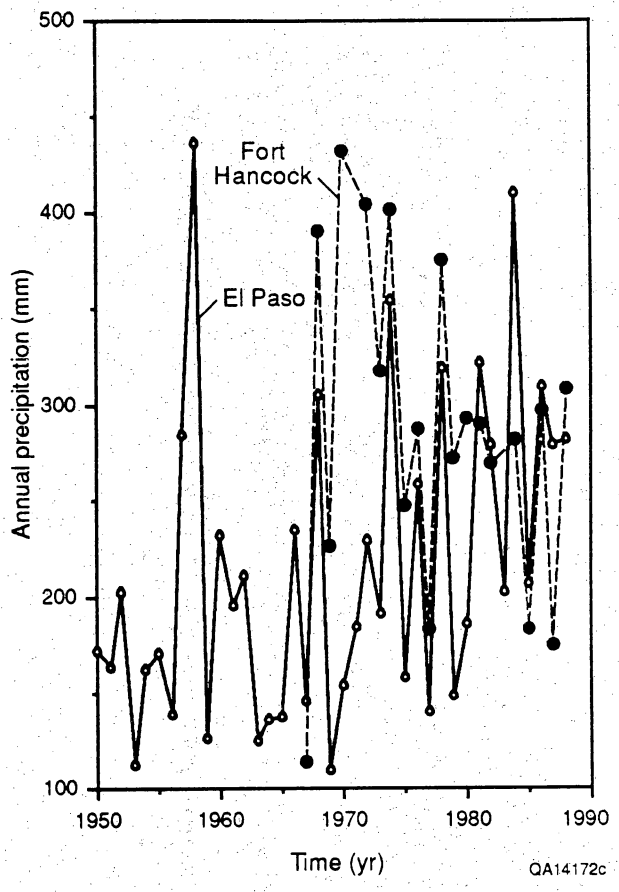

Figure 2. Temporal variations in precipitation recorded in El Paso and Fort Hancock.

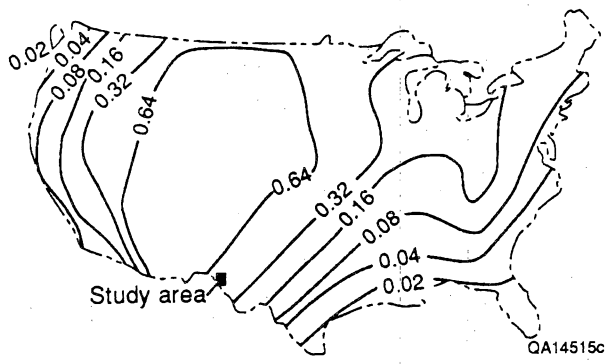

Figure 3. Pre-bomb $^{36}Cl/Cl$ fallout ratios (atoms $^{36}Cl/10^{12}$ atoms Cl) calculated using atmospheric box model (Bentley and others, 1986).

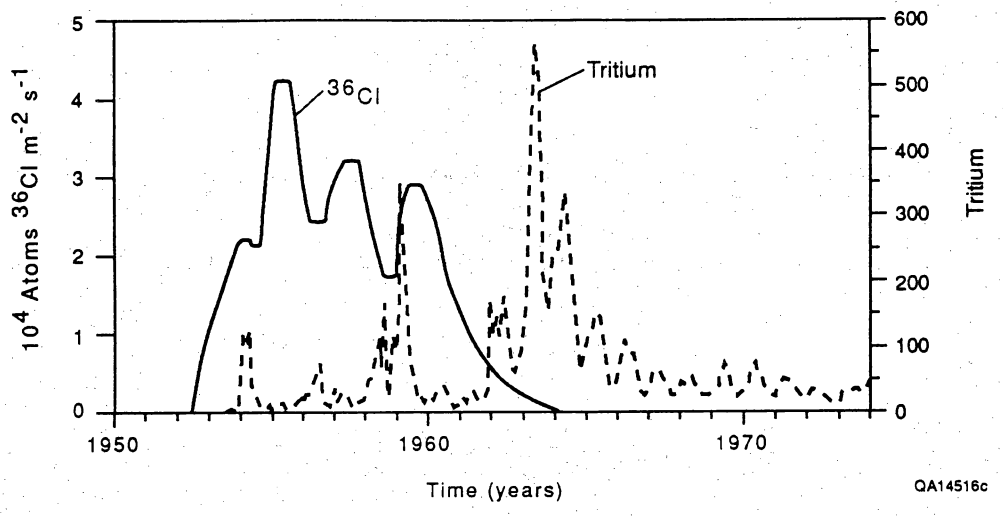

Figure 4. Temporal variations in predicted bomb ^{36}Cl fallout between 30°N and 50°N latitude (Bentley and others, 1986), and in bomb ^{3}H fallout (IAEA, 1983). Decay corrected to 1989.

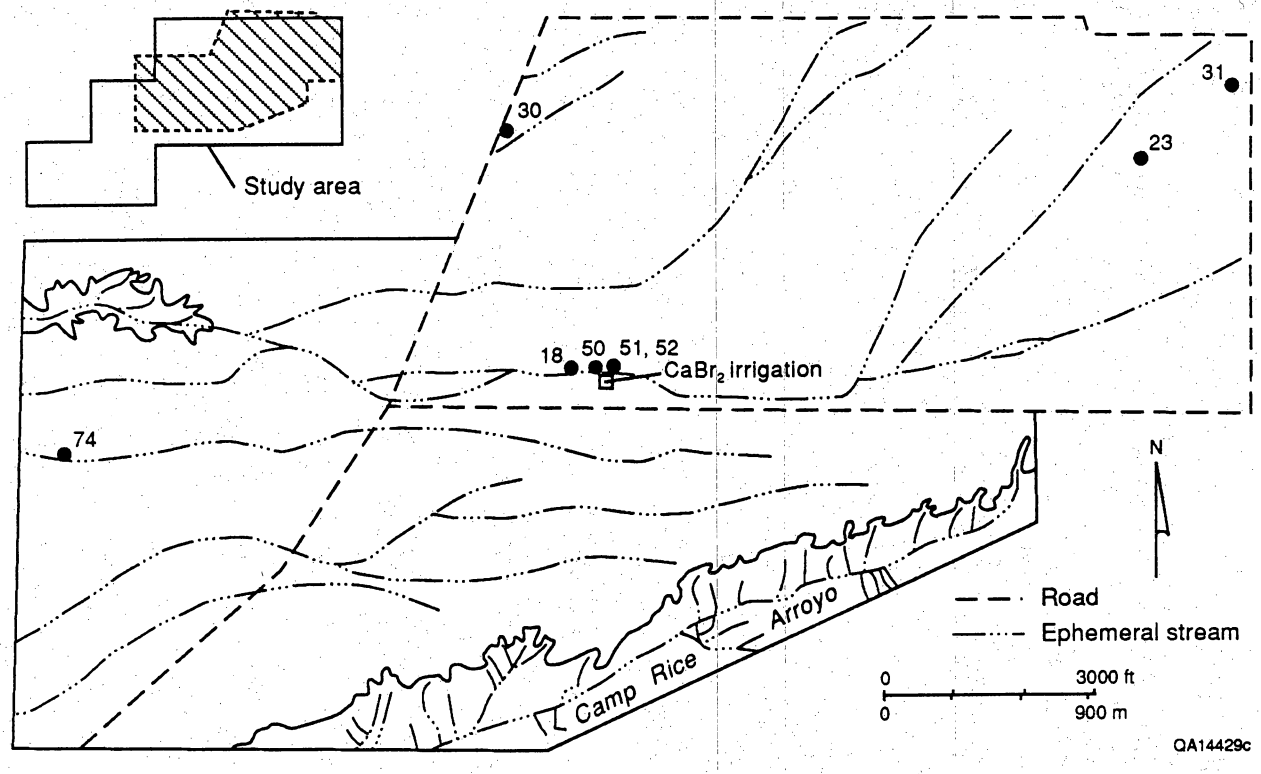

Figure 5. Location of sampled boreholes and of bromide test plot. Samples from these boreholes were analyzed for moisture content and chloride. Samples from borehole 51 were also analyzed for ^{36}Cl, and samples from borehole 52 were also analyzed for ^{3}H.

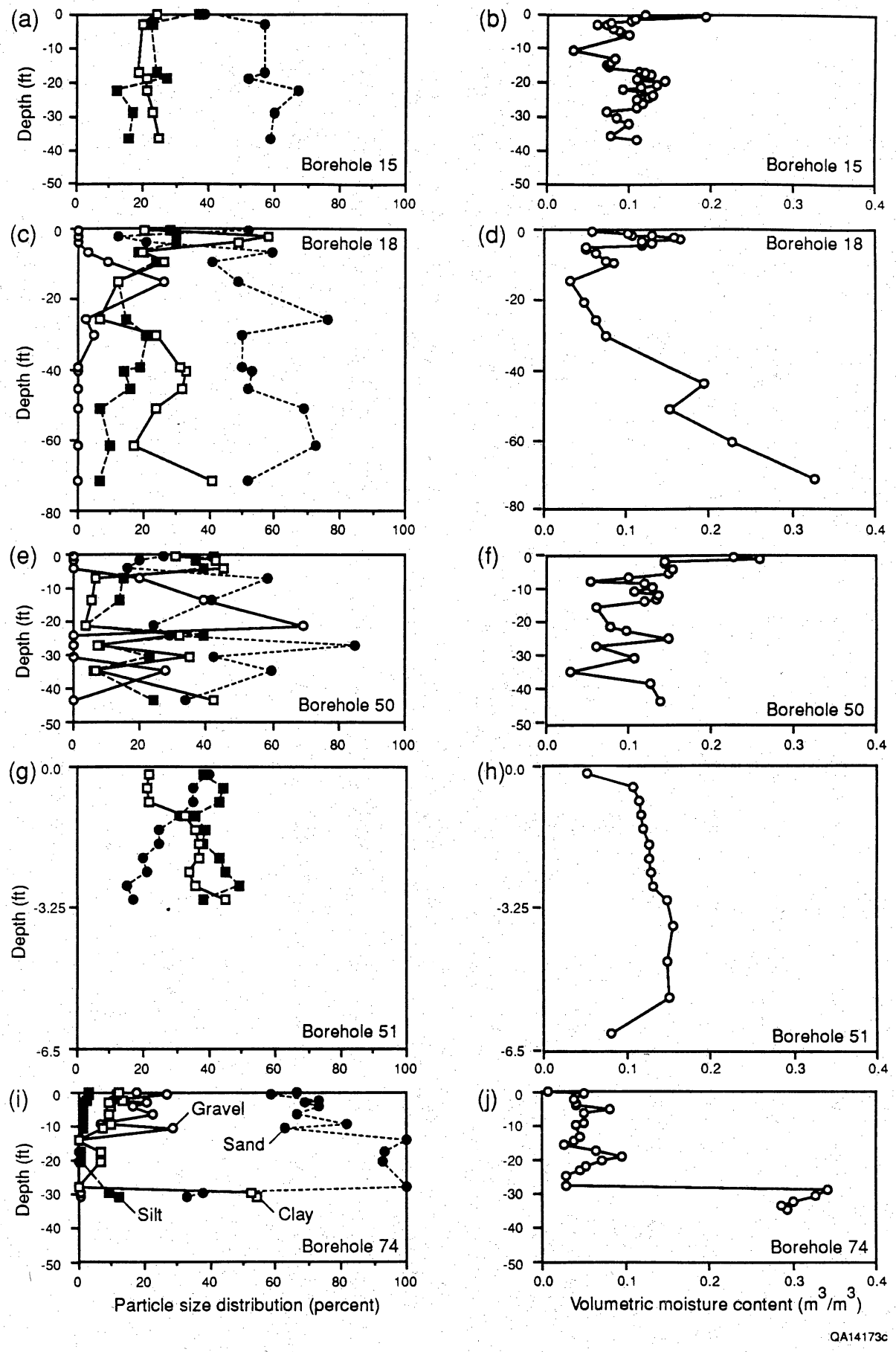

Figure 6. Profiles of grain size and volumetric moisture content of samples from boreholes drilled in stream settings.

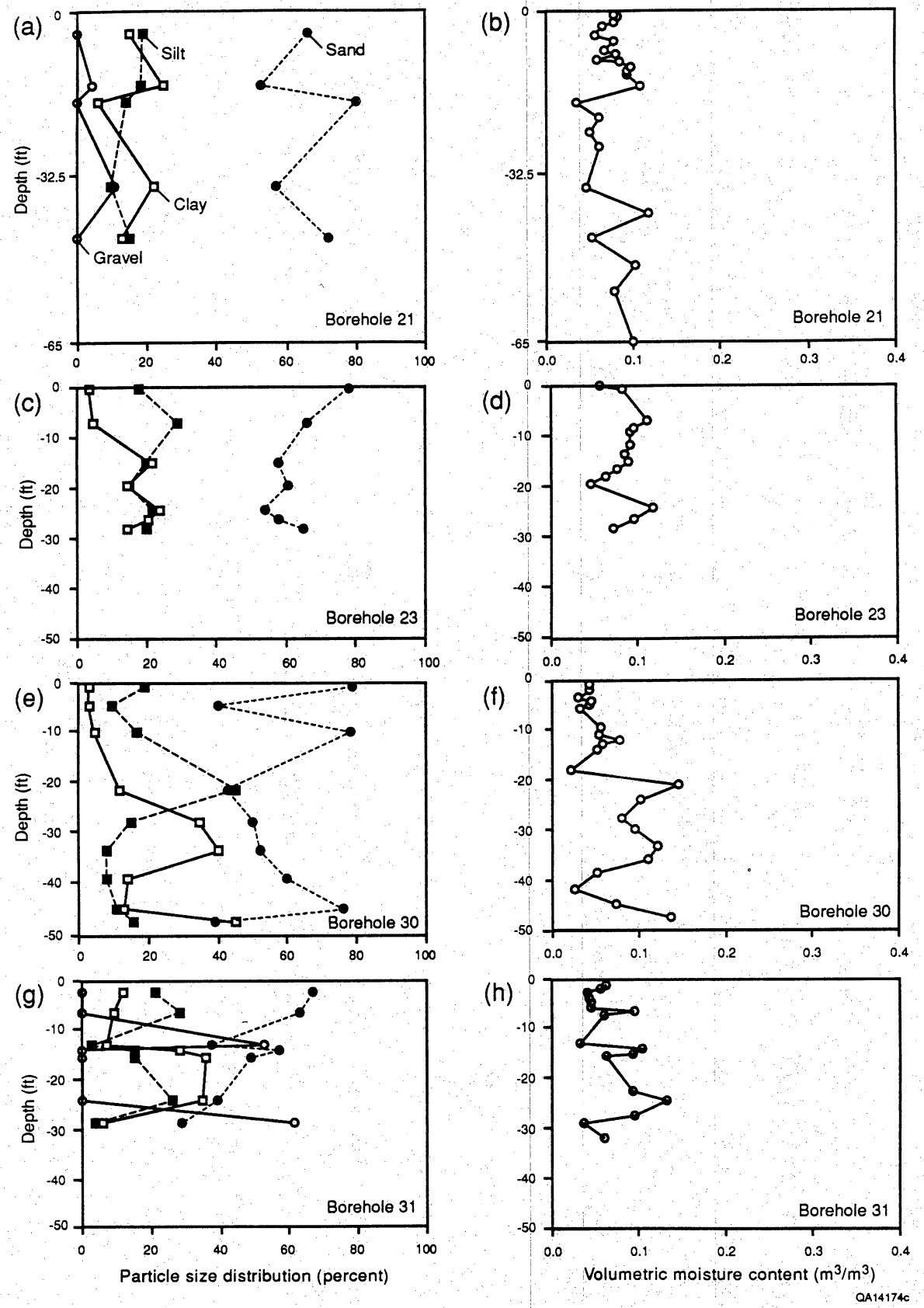

Figure 7. Profiles of grain size and volumetric moisture content of samples from boreholes drilled in interstream settings.

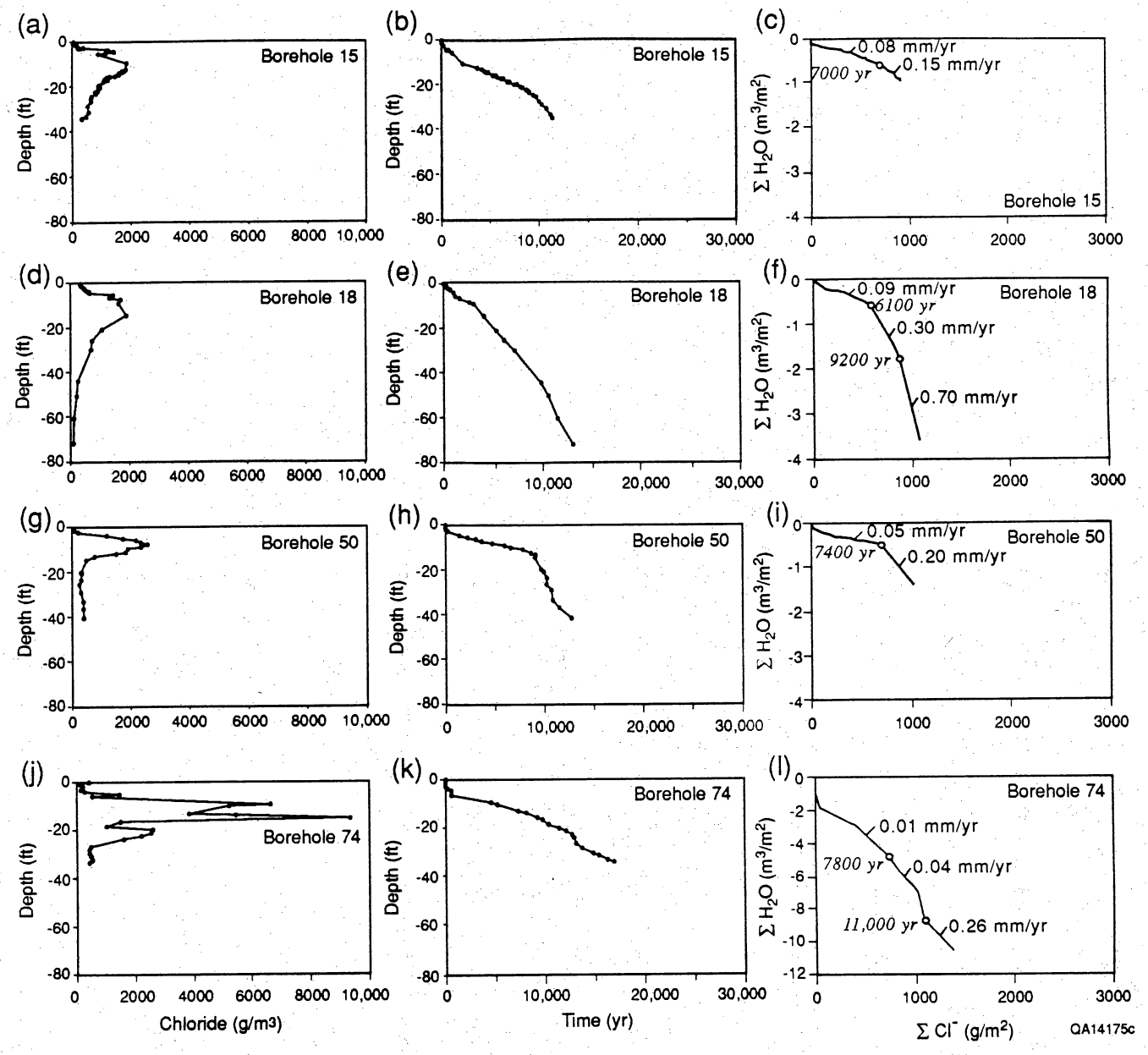

Figure 8. Profiles of chloride concentration and chloride mass-balance age of samples from boreholes drilled in stream settings. Also shown is cumulative chloride versus cumulative water content.

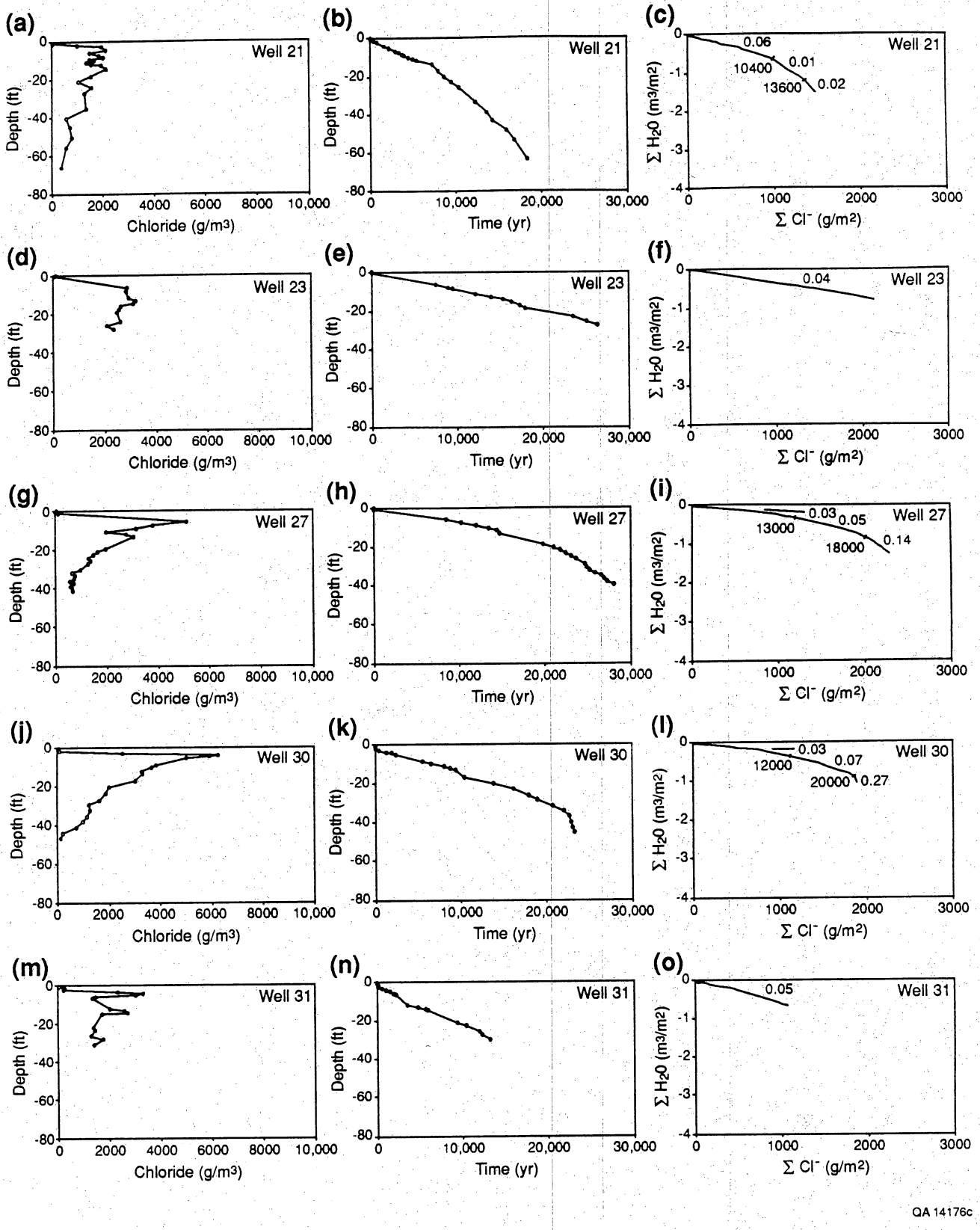

Figure 9. Profiles of chloride concentration and chloride mass-balance age of samples from boreholes drilled in interstream settings. Also shown is cumulative chloride versus cumulative water content.

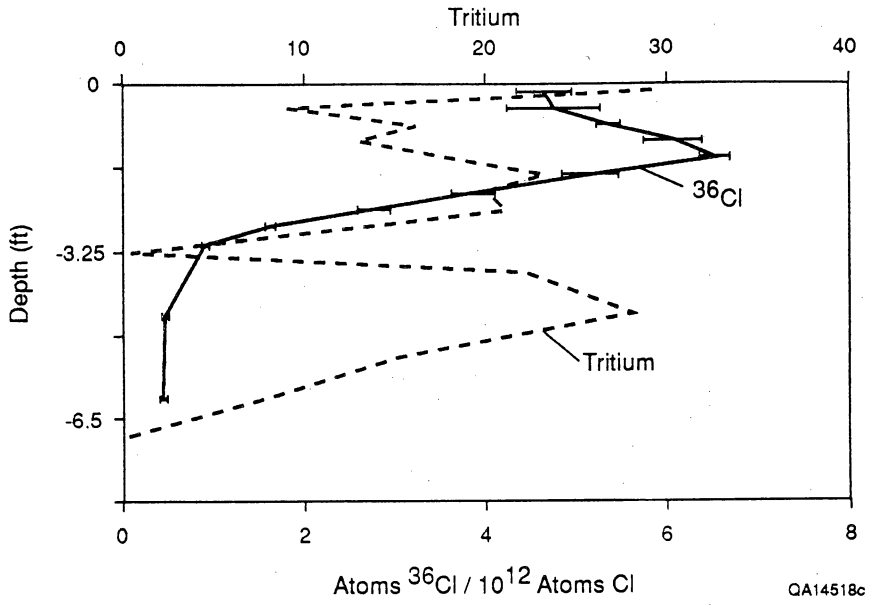

Figure 10. Vertical profile in $^{36}Cl/Cl$ ratios and ^{3}H concentrations. The bars represent 1 standard deviation in the $^{36}Cl/Cl$ ratios. The analytical uncertainty associated with the ^{3}H measurements is ± 8 TU and was omitted for clarity.

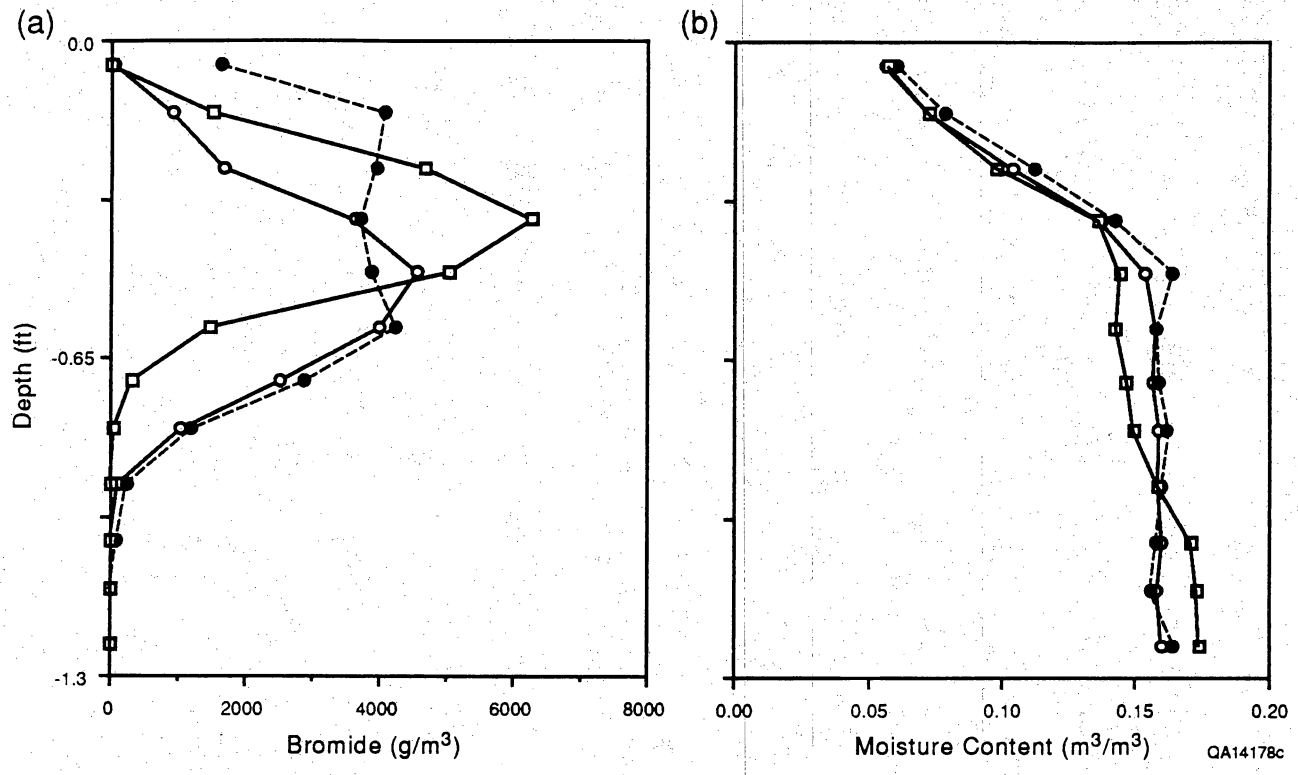

Figure 11. Three profiles of (a) bromide and (b) moisture content sampled within 100 m^2 test plot 1 yr after artificial application of bromide with an irrigation system.

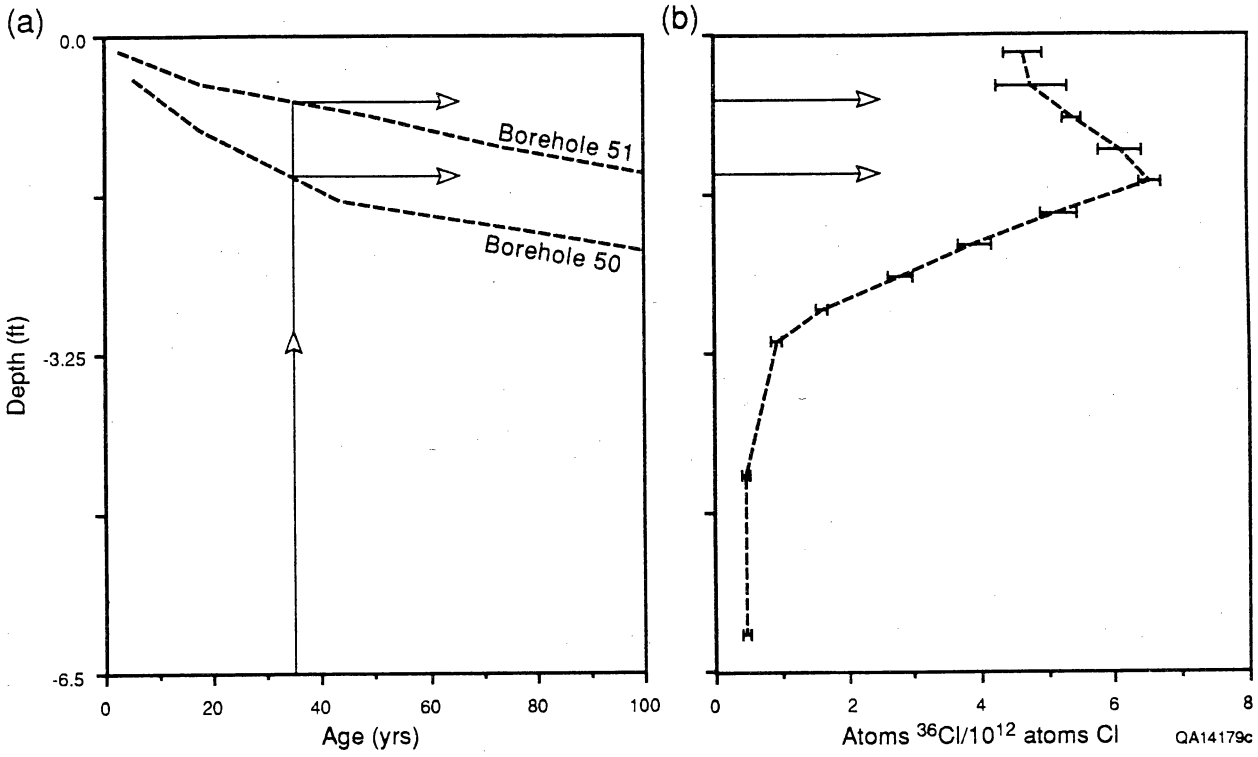

Figure 12. Comparison of the predicted depth of the $^{36}Cl/Cl$ peak based on chloride mass-balance data from boreholes 50 and 51 and the observed peak depth in borehole 51.

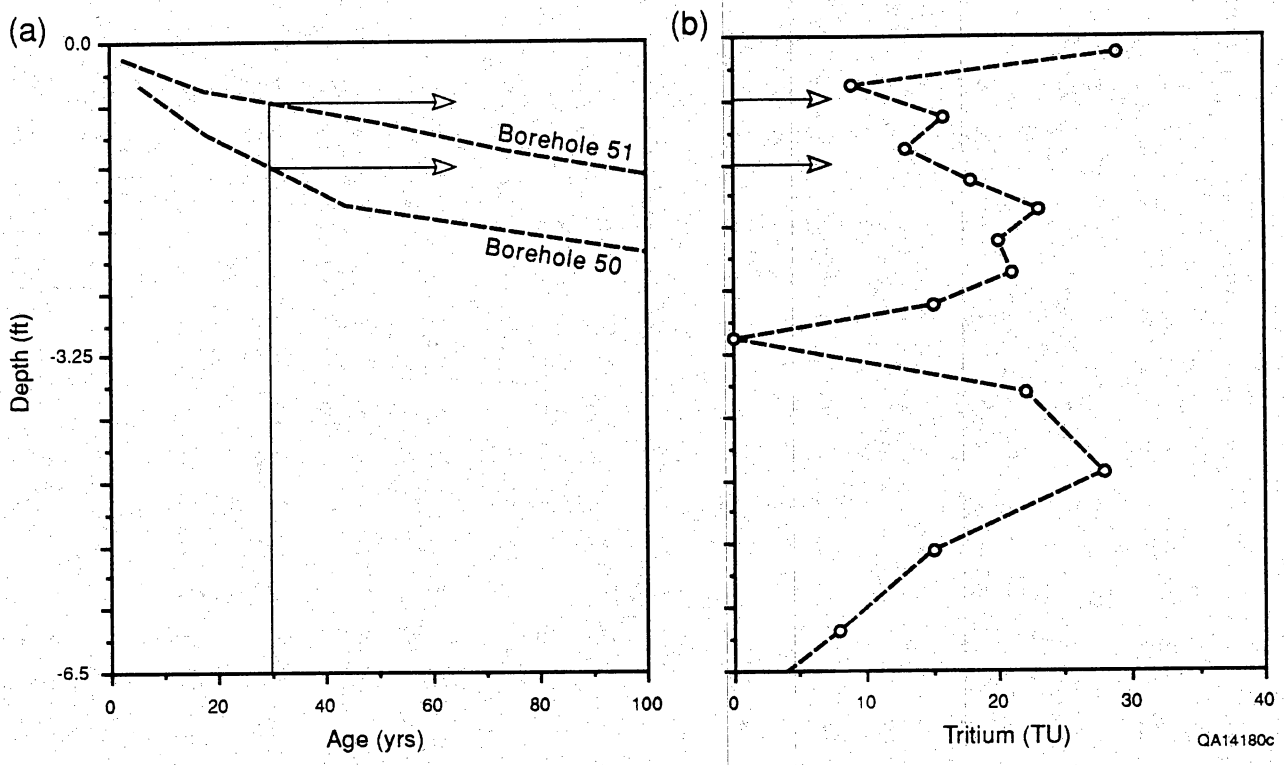

Figure 13. Comparison of the predicted depth of the ^{3}H peak based on chloride mass-balance data from boreholes 50 and 51 and the observed peak depth in borehole 52.

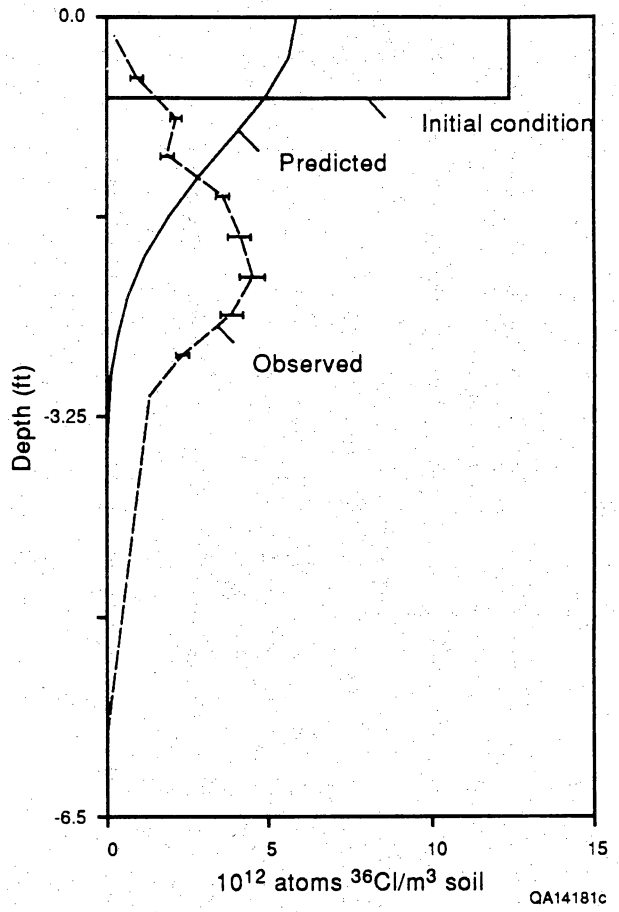

Figure 14. Comparison of the calculated ^{36}Cl profile based on diffusion from the upper 0.2 m and the observed ^{36}Cl profile.

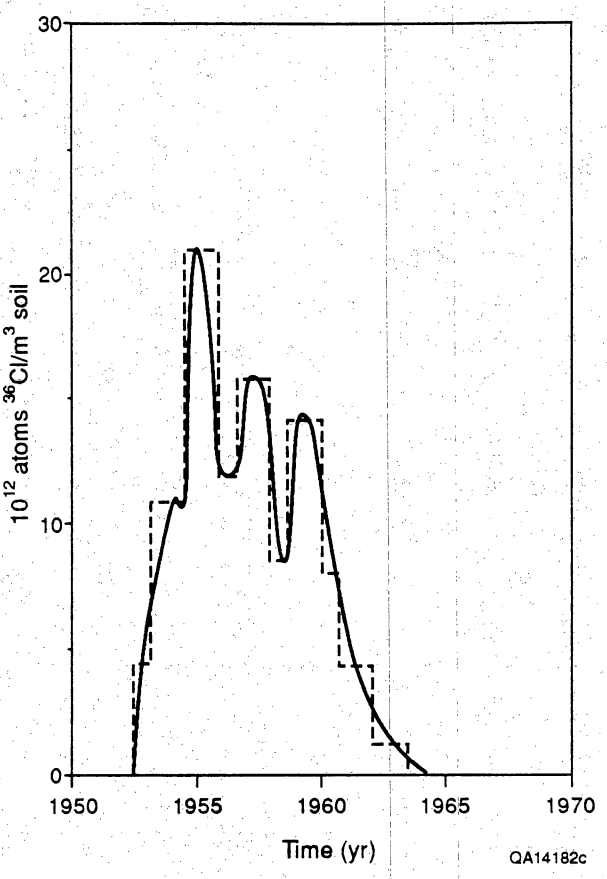

Figure 15. Approximation of the ^{36}Cl fallout with a step function that was used in the analysis of advective-dispersive transport of ^{36}Cl.

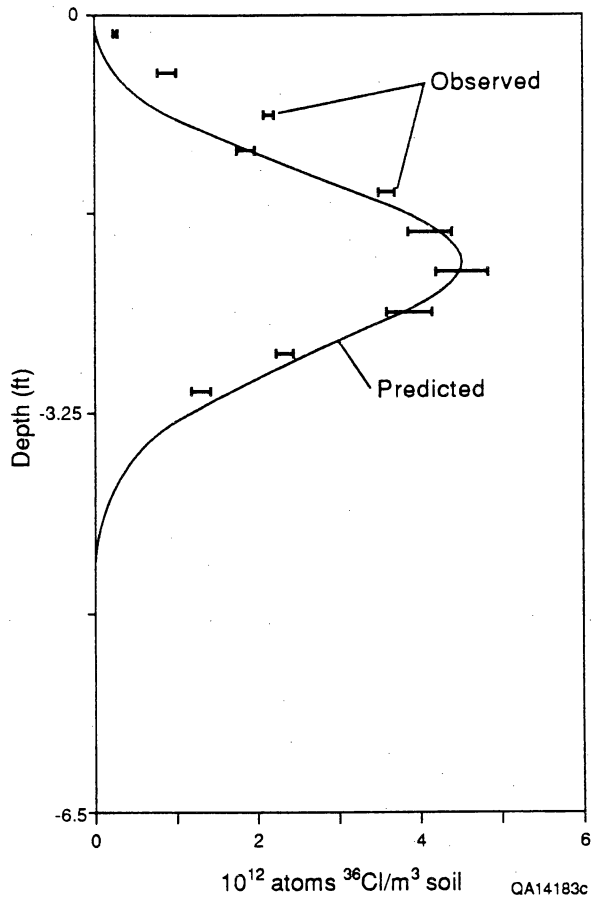

Figure 16. Comparison of the calculated ^{36}Cl profile based on an analytical solution of the advection-dispersion equation and the observed ^{36}Cl profile.

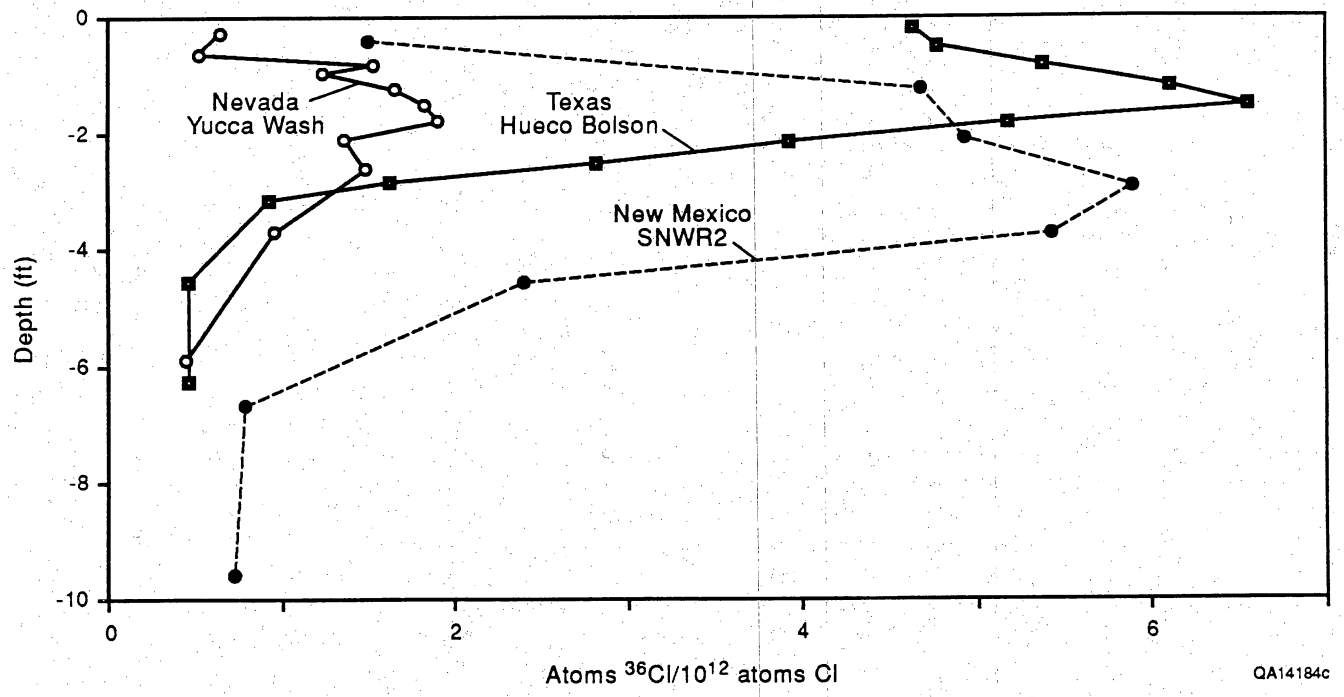

Figure 17. Comparison of $^{36}Cl/Cl$ profiles sampled in Texas, New Mexico (Phillips and others, 1988), and Nevada (Norris and others, 1987).

Table 1. Data on grain size, soil texture, and volumetric moisture content.

Borehole number	Depth (ft)	Gravel (%)	Sand (%)	Silt (%)	Clay (%)	Soil texture	Volumetric moisture content (m^3/m^3)
15	-0.07	0	39	37	24	loam	0.12
	-2.95	0	57	23	20	sandy clay loam	0.06
	-16.90	0	57	24	19	sandy loam	0.12
	-18.77	0	52	27	21	sandy clay loam	0.11
	-21.69	0	67	12	21	sandy clay loam	0.09
	-28.08	0	60	17	23	sandy clay loam	0.07
	-35.83	0	59	16	25	sandy clay loam	0.11
	-0.50	0	52	28	20	sandy clay loam	0.06
	-2.50	0	12	30	58	clay	0.15
	-4.00	0	21	30	49	clay	0.13
	-7.00	3	59	19	19	sandy clay loam	0.06
	-9.75	9	41	24	26	gravelly mud	0.09
	-15.19	26	49	12	13	gravelly muddy sand	0.03
18	-26.50	2	76	15	7	loamy sand	0.06
	-31.00	5	50	21	24	gravelly muddy sand	0.07
	-40.10	0	50	19	31	sandy clay loam	-
	-41.30	0	53	14	33	sandy clay loam	-
	-46.30	0	52	16	32	sandy clay loam	-
	-52.40	0	69	7	24	sandy clay loam	-
	-63.10	0	73	10	17	sandy loam	-
	-73.30	0	52	7	41	sandy clay	0.33
	-4.79	0	66	19	15	sandy loam	0.06
	-14.80	5	53	18	25	sandy clay loam	0.11
21	-18.01	0	80	14	6	loamy sand	0.03
	-35.01	11	57	10	22	gravelly muddy sand	0.04
	-45.01	0	72	15	13	sandy loam	0.05
	-65.72	0	50	22	28	sandy clay loam	0.10
	-0.16	0	78	18	4	loamy sand	0.06
	-7.05	0	66	29	5	sandy loam	0.11
	-14.83	0	58	20	22	sandy clay loam	0.09
23	-19.26	9	61	15	15	sandy loam	0.04
	-24.08	0	54	22	24	sandy clay loam	0.12
	-26.12	0	58	21	21	sandy clay loam	0.10
	-28.08	0	65	20	15	sandy loam	0.07
	-50.85	0	20	37	43	clay	-
	-54.99	0	28	28	44	clay	-
	-0.66	0	79	19	3	loamy sand	0.04
	-4.13	47	40	10	3	muddy sandy gravel	0.05
	-9.35	0	78	17	5	loamy sand	0.06
	-20.64	0	43	45	12	loam	0.15

Table 1 (cont.)

Borehole number	Depth (ft)	Gravel (%)	Sand (%)	Silt (%)	Clay (%)	Soil texture	Volumetric moisture content (m^3/m^3)
30	-27.17	0	50	15	35	sandy clay	0.08
	-32.64	0	52	8	40	sandy clay	0.12
	-37.96	18	60	8	14	gravelly muddy sand	0.05
	-44.16	0	76	11	13	sandy loam	0.07
	-46.65	0	39	16	45	clay	0.14
	-1.94	0	67	21	12	sandy loam	0.06
	-6.14	0	63	28	9	sandy loam	0.10
	-12.43	53	37	3	7	muddy sandy gravel	0.03
31	-13.65	0	57	15	28	sandy clay loam	0.10
	-15.06	0	49	15	36	sandy clay	0.06
	-23.65	0	39	26	35	clay loam	0.13
	-28.15	61	29	4	6	muddy sandy gravel	0.04
	-0.46	0	27	42	31	clay loam	0.23
	-1.71	0	20	37	43	clay	0.14
	-4.20	0	16	39	45	clay	0.15
	-7.19	20	58	15	6	gravelly muddy sand	0.05
	-13.45	39	41	14	5	muddy sandy gravel	0.12
50	-20.54	69	24	3	4	muddy sandy gravel	0.08
	-23.95	0	29	39	32	clay loam	0.15
	-26.44	0	85	8	7	loamy sand	0.06
	-29.95	0	42	23	35	clay loam	0.11
	-34.06	28	60	6	6	loamy sand	0.03
	-42.68	0	34	24	42	clay	0.14
	-0.16	0	40	38	22	loam	0.05
	-0.49	0	35	44	21	loam	0.11
	-0.82	0	35	43	22	loam	0.12
	-1.15	0	31	36	33	clay loam	0.12
	-1.48	0	25	39	36	clay loam	0.12
	-1.80	0	25	38	37	clay loam	0.13
	-2.13	0	20	43	37	silty clay loam	0.13
51	-2.46	0	21	45	34	clay loam	0.13
	-2.79	0	15	49	36	silty clay loam	0.13
	-3.12	0	17	38	45	clay	0.15
	-6.99	7	69	17	7	gravelly muddy sand	0.09
	-7.81	4	55	22	19	sandy clay loam	0.11
	-8.56	3	56	21	19	sandy clay loam	0.11
	-9.38	0	55	24	21	sandy clay loam	0.14
	-11.07	18	61	17	4	gravelly muddy sand	0.09
	-12.71	56	30	10	4	muddy sandy gravel	0.06
	-0.16	18	67	3	12	gravelly muddy sand	0.01
	-0.65	27	59	3	11	gravelly muddy sand	0.05
	-2.17	11	73	2	14	gravelly muddy sand	0.04

Table 1 (cont.)

Borehole number	Depth (ft)	Gravel (%)	Sand (%)	Silt (%)	Clay (%)	Soil texture	Volumetric moisture content (m^3/m^3)
	-3.15	21	69	1	9	gravelly muddy sand	0.04
	-4.13	16	73	2	9	gravelly muddy sand	0.04
	-6.15	23	67	1	9	gravelly muddy sand	0.05
74	-9.15	7	82	1	10	gravelly muddy sand	0.05
	-9.94	29	63	1	7	gravelly muddy sand	0.04
	-14.14	0	100	0	0	sand	0.04
	-16.96	0	93	0	7	sand	0.06
	-20.14	0	93	0	7	sand	0.07
	-27.46	0	100	0	0	sand	0.03
	-28.71	1	38	9	52	clay	0.33
	-30.35	1	33	12	54	clay	0.33

A dash indicates no data.

Table 2. Volumetric moisture content, chloride concentration, moisture flux, specific moisture flux, age, and calculated cumulative chloride and cumulative water content.

Well number	Depth (ft)	Interval thickness (ft)	Moisture content (ft^3/ft^3)	Chloride (mg Cl/kg soil)	Chloride (g Cl/m^3H_2O)	Moisture flux (in/yr)	Specific moisture flux (in/yr)	Age (yr)	Cumulative chloride (g/m^2)	Cumulative H_2O (ft)
	-0.05	0.05	0.12	4	51	0.06	0.53	1	0	0.01
	-0.55	0.50	0.19	5	33	0.10	0.50	13	1	0.10
	-1.05	0.50	0.11	6	85	0.04	0.35	30	2	0.16
	-1.55	0.50	0.10	13	177	0.02	0.18	64	5	0.21
	-2.45	0.90	0.08	11	191	0.02	0.22	114	9	0.28
	-2.95	0.50	0.06	17	401	0.01	0.13	160	13	0.31
	-3.05	0.10	0.07	15	283	0.01	0.16	168	14	0.31
	-4.05	1.00	0.08	70	1,234	0.00	0.03	535	43	0.39
	-4.45	0.40	0.09	89	1,420	0.00	0.03	722	59	0.43
	-5.35	0.90	0.09	75	1,149	0.00	0.03	1,075	87	0.51
	-5.75	0.40	0.10	64	910	0.00	0.04	1,210	98	0.55
	-10.33	4.58	0.03	41	1,858	0.00	0.06	2,191	178	0.69
	-12.95	2.62	0.08	108	1,820	0.00	0.02	3,678	299	0.91
	-13.75	0.80	0.08	95	1,720	0.00	0.02	4,077	331	0.97
15	-14.35	0.60	0.08	93	1,728	0.00	0.02	4,370	355	1.02
	-14.75	0.40	0.07	84	1,603	0.00	0.03	4,547	369	1.04
	-15.05	0.30	0.08	86	1,595	0.00	0.03	4,683	380	1.07
	-16.05	1.00	0.11	119	1,491	0.00	0.02	5,307	431	1.18
	-16.45	0.40	0.11	106	1,311	0.00	0.02	5,530	449	1.22
	-16.90	0.45	0.12	102	1,203	0.00	0.02	5,771	469	1.28
	-17.50	0.60	0.13	102	1,137	0.00	0.02	6,094	495	1.35
	-17.90	0.40	0.12	107	1,220	0.00	0.02	6,318	513	1.40
	-18.75	0.85	0.11	88	1,119	0.00	0.03	6,714	545	1.50
	-19.15	0.40	0.14	110	1,076	0.00	0.02	6,945	564	1.55
	-20.35	1.20	0.13	92	958	0.00	0.02	7,526	611	1.72
	-20.75	0.40	0.12	76	920	0.00	0.03	7,686	624	1.76
	-21.68	0.93	0.09	64	958	0.00	0.04	7,999	649	1.85

Table 2 (cont.)

Well number	Depth (ft)	Interval thickness (ft)	Moisture content (ft^3/ft^3)	Chloride (mg Cl/kg soil)	Chloride (g Cl/m^3H_2O)	Moisture flux (in/yr)	Specific moisture flux (in/yr)	Age (yr)	Cumulative chloride (g/m^2)	Cumulative H_2O (ft)
	-22.08	0.40	0.11	74	901	0.00	0.03	8,153	662	1.89
	-23.20	1.12	0.13	81	881	0.00	0.03	8,630	701	2.04
	-23.60	0.40	0.12	70	789	0.00	0.03	8,776	713	2.09
	-24.25	0.65	0.11	65	831	0.00	0.04	8,997	731	2.16
	-25.35	1.10	0.12	56	677	0.00	0.04	9,322	757	2.29
15	-26.50	1.15	0.11	52	661	0.00	0.04	9,635	782	2.41
	-28.10	1.60	0.07	34	633	0.01	0.07	9,919	805	2.53
	-29.95	1.85	0.09	34	553	0.01	0.07	10,249	832	2.69
	-31.65	1.70	0.10	41	573	0.01	0.06	10,613	862	2.86
	-34.68	3.03	0.08	27	495	0.01	0.08	11,051	897	3.10
	-35.83	1.15	0.11	27	340	0.01	0.09	11,211	910	3.22
	-0.50	0.50	0.06	15	351	0.01	0.15	39	3	0.03
	-1.00	0.50	0.10	26	357	0.01	0.09	107	9	0.08
	-1.50	0.50	0.13	35	376	0.01	0.07	199	16	0.15
	-2.00	0.50	0.11	31	409	0.01	0.07	282	23	0.20
	-2.50	0.50	0.16	49	436	0.01	0.05	411	33	0.28
	-3.00	0.50	0.16	56	479	0.01	0.04	558	45	0.36
	-3.50	0.50	0.12	43	506	0.01	0.05	671	54	0.42
	-4.00	0.50	0.13	53	563	0.01	0.04	809	66	0.49
	-4.50	0.50	0.12	55	640	0.00	0.04	953	77	0.54
18	-5.00	0.50	0.05	24	649	0.00	0.09	1,016	83	0.57
	-6.00	1.00	0.05	54	1,455	0.00	0.04	1,298	105	0.62
	-7.00	1.00	0.06	61	1,335	0.00	0.04	1,617	131	0.69
	-9.00	2.00	0.08	93	1,705	0.00	0.02	2,593	211	0.84
	-9.75	0.75	0.09	100	1,637	0.00	0.02	2,987	243	0.90
	-15.20	5.45	0.03	41	1,921	0.00	0.06	4,174	339	1.07
	-21.50	6.30	0.05	36	1,051	0.00	0.06	5,351	434	1.37
	-26.50	5.00	0.06	33	744	0.00	0.07	6,223	505	1.68
	-31.00	4.50	0.07	38	716	0.00	0.06	7,122	578	2.01
	-45.20	14.20	0.19	36	262	0.01	0.06	9,833	798	4.77

Table 2 (cont.)

Well number	Depth (ft)	Interval thickness (ft)	Moisture content (ft^3/ft^3)	Chloride (mg Cl/kg soil)	Chloride (g Cl/m^3H_2O)	Moisture flux (in/yr)	Specific moisture flux (in/yr)	Age (yr)	Cumulative chloride (g/m^2)	Cumulative H_2O (ft)
	-52.30	7.10	0.15	25	225	0.01	0.09	10,752	873	5.85
18	-62.20	9.90	0.23	16	101	0.03	0.14	11,601	942	8.09
	-73.40	11.20	0.33	25	106	0.03	0.09	13,052	1060	11.75
	-0.75	0.75	0.08	3	57	0.06	0.72	13	1	0.06
	-1.00	0.25	0.08	3	45	0.07	0.87	16	1	0.08
	-2.25	1.25	0.08	56	1,022	0.00	0.04	383	31	0.17
	-3.00	0.75	0.07	93	1,966	0.00	0.02	751	61	0.22
	-4.80	1.80	0.06	84	2,114	0.00	0.03	1,545	125	0.32
	-6.00	1.20	0.08	81	1,476	0.00	0.03	2,055	167	0.42
	-7.80	1.80	0.07	90	1,860	0.00	0.03	2,908	236	0.54
	-8.50	0.70	0.08	115	2,027	0.00	0.02	3,330	270	0.59
	-9.50	1.00	0.06	63	1,484	0.00	0.04	3,659	297	0.65
	-10.00	0.50	0.09	102	1,662	0.00	0.02	3,927	319	0.70
	-11.00	1.00	0.10	94	1,351	0.00	0.02	4,421	359	0.79
21	-11.90	0.90	0.09	102	1,524	0.00	0.02	4,906	398	0.88
	-12.50	0.60	0.09	128	1,943	0.00	0.02	5,310	431	0.93
	-14.80	2.30	0.11	163	2,121	0.00	0.01	7,280	591	1.18
	-18.00	3.20	0.03	37	1,538	0.00	0.06	7,900	641	1.29
	-21.00	3.00	0.06	46	1,069	0.00	0.05	8,624	700	1.47
	-24.00	3.00	0.05	56	1,568	0.00	0.04	9,506	772	1.62
	-27.00	3.00	0.06	56	1,297	0.00	0.04	10,394	844	1.80
	-35.00	8.00	0.04	43	1,369	0.00	0.05	12,216	992	2.16
	-40.30	5.30	0.12	50	599	0.01	0.05	13,623	1106	2.78
	-45.00	4.70	0.05	27	726	0.00	0.08	14,289	1160	3.03
	-50.35	5.35	0.10	58	804	0.00	0.04	15,916	1292	3.57
	-55.60	5.25	0.08	32	571	0.01	0.07	16,789	1363	3.97
	-65.70	10.10	0.10	28	391	0.01	0.08	18,267	1483	4.98
	-0.15	0.15	0.06	5	124	0.03	0.46	4	0	0.01
23	-0.65	0.50	0.08	4	61	0.05	0.65	13	1	0.05
	-7.05	6.40	0.11	224	2,885	0.00	0.01	7,535	612	0.74

Table 2 (cont.)

Well number	Depth (ft)	Interval thickness (ft)	Moisture content (ft^3/ft^3)	Chloride (mg Cl/kg soil)	Chloride (g Cl/m^3H_2O)	Moisture flux (in/yr)	Specific moisture flux (in/yr)	Age (yr)	Cumulative chloride (g/m^2)	Cumulative H_2O (ft)
	-8.45	1.40	0.09	192	2,851	0.00	0.01	8,949	727	0.88
	-8.95	0.50	0.09	183	2,857	0.00	0.01	9,430	766	0.92
	-11.70	2.75	0.09	187	2,959	0.00	0.01	12,128	985	1.16
	-13.45	1.75	0.08	194	3,194	0.00	0.01	13,909	1129	1.31
	-14.82	1.37	0.09	194	3,114	0.00	0.01	15,312	1243	1.43
23	-16.25	1.43	0.08	140	2,614	0.00	0.02	16,364	1329	1.54
	-17.80	1.55	0.06	113	2,560	0.00	0.02	17,287	1404	1.64
	-19.25	1.45	0.04	77	2,470	0.00	0.03	17,875	1451	1.70
	-24.08	4.83	0.12	222	2,626	0.00	0.01	23,495	1908	2.27
	-26.10	2.03	0.10	150	2,110	0.00	0.02	25,087	2037	2.47
	-28.10	2.00	0.07	122	2,342	0.00	0.02	26,369	2141	2.62
	-0.15	0.15	0.13	5	58	0.06	0.43	4	0	0.02
	-0.65	0.50	0.14	4	35	0.09	0.65	13	1	0.09
	-1.15	0.50	0.06	5	112	0.03	0.45	27	2	0.12
	-6.30	5.15	0.09	312	5,121	0.00	0.01	8,475	688	0.56
	-7.75	1.45	0.09	233	3,819	0.00	0.01	10,253	833	0.69
	-9.25	1.50	0.10	224	3,145	0.00	0.01	12,019	976	0.84
	-10.70	1.45	0.10	183	2,543	0.00	0.01	13,412	1089	0.98
	-12.20	1.50	0.06	123	2,768	0.00	0.02	14,385	1168	1.07
	-13.65	1.45	0.02	40	3,051	0.00	0.06	14,690	1193	1.10
27	-19.65	6.00	0.12	164	1,988	0.00	0.01	19,856	1612	1.79
	-21.35	1.70	0.12	139	1,660	0.00	0.02	21,096	1713	1.99
	-22.70	1.35	0.10	107	1,496	0.00	0.02	21,859	1775	2.13
	-24.35	1.65	0.08	75	1,318	0.00	0.03	22,507	1828	2.26
	-25.80	1.45	0.08	79	1,389	0.00	0.03	23,108	1876	2.37
	-27.25	1.45	0.08	76	1,294	0.00	0.03	23,687	1923	2.49
	-30.20	2.95	0.09	67	1,002	0.00	0.03	24,730	2008	2.77
	-31.70	1.50	0.05	24	677	0.00	0.10	24,918	2023	2.85
	-33.25	1.55	0.07	36	761	0.00	0.06	25,213	2047	2.95
	-34.70	1.45	0.18	95	748	0.00	0.02	25,934	2106	3.21

Table 2 (cont.)

Well number	Depth (ft)	Interval thickness (ft)	Moisture content (ft^3/ft^3)	Chloride (mg Cl/kg soil)	Chloride (g Cl/m^3H_2O)	Moisture flux (in/yr)	Specific moisture flux (in/yr)	Age (yr)	Cumulative chloride (g/m^2)	Cumulative H_2O (ft)
	-36.25	1.55	0.20	80	566	0.01	0.03	26,584	2159	3.51
	-37.60	1.35	0.10	51	710	0.00	0.04	26,945	2188	3.65
27	-39.30	1.70	0.09	37	586	0.01	0.06	27,279	2215	3.80
	-39.50	0.20	0.13	60	634	0.01	0.04	27,342	2220	3.82
	-41.05	1.55	0.19	94	677	0.00	0.02	28,106	2282	4.13
	-0.65	0.65	0.04	2	79	0.04	0.92	8	1	0.03
	-1.95	1.30	0.05	3	104	0.03	0.68	31	3	0.09
	-3.35	1.40	0.03	57	2,549	0.00	0.04	449	36	0.13
	-4.15	0.80	0.05	209	6,262	0.00	0.01	1,327	108	0.17
	-4.65	0.50	0.04	186	5,944	0.00	0.01	1,815	147	0.19
	-5.45	0.80	0.03	113	5,035	0.00	0.02	2,292	186	0.22
	-9.35	3.90	0.06	156	3,856	0.00	0.01	5,490	446	0.44
	-10.65	1.30	0.05	144	3,679	0.00	0.02	6,473	526	0.51
	-11.75	1.10	0.08	281	5,045	0.00	0.01	8,096	657	0.59
	-12.65	0.90	0.06	141	3,342	0.00	0.02	8,761	711	0.65
30	-13.65	1.00	0.05	125	3,319	0.00	0.02	9,417	765	0.70
	-17.55	3.90	0.02	47	3,040	0.00	0.05	10,379	843	0.78
	-20.65	3.10	0.15	213	2,024	0.00	0.01	13,854	1125	1.24
	-23.65	3.00	0.10	145	1,955	0.00	0.02	16,142	1311	1.55
	-27.15	3.50	0.08	95	1,635	0.00	0.02	17,893	1453	1.84
	-29.65	2.50	0.10	87	1,249	0.00	0.03	19,031	1545	2.08
	-32.65	3.00	0.12	111	1,269	0.00	0.02	20,779	1687	2.45
	-35.35	2.70	0.11	95	1,182	0.00	0.02	22,121	1796	2.75
	-37.95	2.60	0.05	38	1,012	0.00	0.06	22,638	1838	2.89
	-41.25	3.30	0.03	14	743	0.00	0.16	22,885	1858	2.97
	-44.15	2.90	0.07	12	223	0.01	0.19	23,067	1873	3.19
	-46.65	2.50	0.14	14	146	0.02	0.16	23,256	1888	3.54
	-0.95	0.95	0.06	3	70	0.05	0.73	16	1	0.06
31	-1.95	1.00	0.06	12	297	0.01	0.19	80	6	0.12
	-2.65	0.70	0.04	7	257	0.01	0.31	107	9	0.15

Table 2 (cont.)

Well number	Depth (ft)	Interval thickness (ft)	Moisture content (ft^3/ft^3)	Chloride (mg Cl/kg soil)	Chloride (g Cl/m^3H_2O)	Moisture flux (in/yr)	Specific moisture flux (in/yr)	Age (yr)	Cumulative chloride (g/m^2)	Cumulative H_2O (ft)
	-3.55	0.90	0.04	74	2,363	0.00	0.03	459	37	0.19
	-4.50	0.95	0.04	107	3,345	0.00	0.02	994	81	0.23
	-5.35	0.85	0.04	96	3,047	0.00	0.02	1,424	116	0.27
	-6.15	0.80	0.10	101	1,484	0.00	0.02	1,849	150	0.34
	-6.80	0.65	0.06	60	1,362	0.00	0.04	2,053	167	0.38
	-12.45	5.65	0.03	49	2,048	0.00	0.05	3,519	286	0.57
31	-13.65	1.20	0.10	192	2,602	0.00	0.01	4,728	384	0.70
	-14.65	1.00	0.09	183	2,761	0.00	0.01	5,691	462	0.79
	-15.05	0.40	0.06	78	1,728	0.00	0.03	5,855	475	0.81
	-22.10	7.05	0.09	94	1,405	0.00	0.02	9,336	758	1.47
	-23.65	1.55	0.13	137	1,449	0.00	0.02	10,451	849	1.68
	-26.65	3.00	0.10	92	1,321	0.00	0.02	11,896	966	1.97
	-28.15	1.50	0.04	46	1,719	0.00	0.05	12,256	995	2.03
	-31.05	2.90	0.06	61	1,428	0.00	0.04	13,186	1071	2.20
	-0.45	0.45	0.23	2	14	0.22	0.98	5	0	0.10
	-0.95	0.50	0.26	5	26	0.12	0.48	18	1	0.23
	-1.70	0.75	0.14	7	65	0.05	0.35	44	4	0.34
	-2.45	0.75	0.14	22	216	0.01	0.10	131	11	0.44
	-4.20	1.75	0.15	133	1,211	0.00	0.02	1,354	110	0.71
	-5.20	1.00	0.15	183	1,736	0.00	0.01	2,317	188	0.86
	-6.20	1.00	0.10	156	2,179	0.00	0.01	3,137	255	0.96
	-7.20	1.00	0.05	90	2,349	0.00	0.03	3,609	293	1.02
50	-8.20	1.00	0.12	220	2,569	0.00	0.01	4,764	387	1.14
	-9.20	1.00	0.13	216	2,365	0.00	0.01	5,901	479	1.26
	-10.20	1.00	0.11	146	1,904	0.00	0.02	6,671	542	1.37
	-11.45	1.25	0.14	180	1,849	0.00	0.01	7,855	638	1.54
	-12.45	1.00	0.13	143	1,502	0.00	0.02	8,605	699	1.67
	-13.45	1.00	0.12	65	770	0.00	0.04	8,947	726	1.79
	-14.65	1.20	0.06	21	486	0.01	0.11	9,078	737	1.86
	-20.55	5.90	0.08	19	341	0.01	0.12	9,668	785	2.33

Table 2 (cont.)

Well number	Depth (ft)	Interval thickness (ft)	Moisture content (ft^3/ft^3)	Chloride (mg Cl/kg soil)	Chloride (g Cl/m^3H_2O)	Moisture flux (in/yr)	Specific moisture flux (in/yr)	Age (yr)	Cumulative chloride (g/m^2)	Cumulative H_2O (ft)
	-21.55	1.00	0.10	24	335	0.01	0.10	9,792	795	2.42
	-23.95	2.40	0.15	33	310	0.01	0.07	10,211	829	2.78
	-26.45	2.50	0.06	10	245	0.01	0.22	10,348	840	2.93
50	-29.95	3.50	0.11	24	311	0.01	0.10	10,784	876	3.31
	-34.05	4.10	0.03	8	381	0.01	0.28	10,960	890	3.43
	-37.55	3.50	0.13	35	384	0.01	0.07	11,602	942	3.87
	-42.70	5.15	0.14	40	403	0.01	0.06	12,692	1031	4.59
	-0.16	0.16	0.05	3	74	0.04	0.82	2	0	0.01
	-0.49	0.33	0.11	9	115	0.03	0.26	18	1	0.04
	-0.82	0.33	0.12	19	224	0.01	0.12	50	4	0.08
	-1.15	0.33	0.12	14	165	0.02	0.16	74	6	0.12
	-1.48	0.33	0.12	25	289	0.01	0.09	117	9	0.16
	-1.80	0.33	0.13	37	405	0.01	0.06	181	15	0.20
	-2.13	0.33	0.13	56	612	0.01	0.04	277	22	0.24
	-2.46	0.33	0.13	71	760	0.00	0.03	399	32	0.29
	-2.79	0.33	0.13	88	934	0.00	0.03	550	45	0.33
	-3.12	0.33	0.15	127	1,193	0.00	0.02	769	62	0.38
	-3.69	0.57	0.16	165	1,474	0.00	0.01	1,266	103	0.47
51	-4.51	0.82	0.15	230	2,175	0.00	0.01	2,256	183	0.59
	-5.33	0.82	0.15	281	2,580	0.00	0.01	3,468	282	0.72
	-6.15	0.82	0.08	127	2,169	0.00	0.02	4,015	326	0.78
	-6.97	0.82	0.09	139	2,276	0.00	0.02	4,612	374	0.85
	-7.79	0.82	0.11	172	2,215	0.00	0.01	5,355	435	0.94
	-8.55	0.76	0.12	167	1,998	0.00	0.01	6,026	489	1.03
	-9.38	0.82	0.14	150	1,548	0.00	0.02	6,671	542	1.14
	-10.25	0.88	0.09	83	1,277	0.00	0.03	7,055	573	1.22
	-11.07	0.82	0.09	66	1,063	0.00	0.03	7,341	596	1.29
	-11.89	0.82	0.10	72	1,048	0.00	0.03	7,650	621	1.37
	-12.71	0.82	0.06	38	840	0.00	0.06	7,814	635	1.42
	-13.53	0.82	0.07	27	568	0.01	0.08	7,930	644	1.48

Table 2 (cont.)

Well number	Depth (ft)	Interval thickness (ft)	Moisture content (ft^3/ft^3)	Chloride (mg Cl/kg soil)	Chloride (g Cl/m^3H_2O)	Moisture flux (in/yr)	Specific moisture flux (in/yr)	Age (yr)	Cumulative chloride (g/m^2)	Cumulative H_2O (ft)
	-0.15	0.15	0.01	3	431	0.01	0.83	2	0	0.00
	-0.65	0.50	0.05	4	102	0.03	0.62	12	1	0.03
	-2.15	1.50	0.04	6	231	0.01	0.37	61	5	0.08
	-3.15	1.00	0.04	5	168	0.02	0.46	87	7	0.12
	-4.15	1.00	0.04	8	286	0.01	0.27	131	11	0.17
	-5.10	0.95	0.08	84	1,445	0.00	0.03	552	45	0.24
	-6.15	1.05	0.05	21	565	0.01	0.11	667	54	0.30
	-9.15	3.00	0.05	243	6,639	0.00	0.01	4,500	365	0.45
	-9.95	0.80	0.04	150	5,216	0.00	0.02	5,130	417	0.48
	-13.15	3.20	0.05	124	3,842	0.00	0.02	7,222	586	0.63
	-14.15	1.00	0.04	152	5,453	0.00	0.02	8,021	651	0.67
74	-15.40	1.25	0.03	176	9,343	0.00	0.01	9,175	745	0.70
	-16.95	1.55	0.06	69	1,497	0.00	0.03	9,734	790	0.80
	-18.75	1.80	0.10	70	1,030	0.00	0.03	10,400	844	0.97
	-20.15	1.40	0.07	136	2,630	0.00	0.02	11,400	926	1.07
	-21.65	1.50	0.05	98	2,568	0.00	0.02	12,175	989	1.15
	-22.95	1.30	0.04	71	2,233	0.00	0.03	12,661	1028	1.21
	-24.35	1.40	0.03	33	1,638	0.00	0.07	12,901	1048	1.25
	-27.45	3.10	0.03	10	477	0.01	0.23	13,060	1060	1.34
	-28.70	1.25	0.33	110	459	0.01	0.02	13,780	1119	1.76
	-30.35	1.65	0.33	106	454	0.01	0.02	14,701	1194	2.30
	-31.70	1.35	0.30	110	507	0.01	0.02	15,479	1257	2.71
	-33.15	1.45	0.29	110	536	0.01	0.02	16,314	1325	3.12
	-34.35	1.20	0.29	96	456	0.01	0.02	16,918	1374	3.47

Table 3. Geomorphic setting and characteristics of chloride profiles.

Borehole no.	Geomorphic setting	Maximum Cl (g/m3)	Depth z1 (ft)	Depth z2 (ft)	Depth z3 (ft)	Specific moisture flux (in/yr) Range	Mean	Number of samples
15	stream	1860	1.0	10.5	> 36	1.6–7.2	3.1	38
18	stream	1920		15.1	62	2.0–11.8	5.4	22
50	stream	2570	1.6	8.2	20	1.0–23.3	6.4	23
51	stream	2580	0.2	5.2	> 13	0.0–7.2	0.8	23
74	stream	9340	4.3	15.4	28	0.7–19.7	3.1	24
21	interstream	2120	1.0	14.8	> 66	1.3–7.2	3.5	24
23	interstream	3190	0.7	13.5	> 30	1.0–2.6	1.2	14
27	interstream	5120	1.3	6.2	33	1.0–7.9	2.8	24
30	interstream	6260	2.0	4.3	46	0.7–16.1	4.0	22
31	interstream	3350	1.0	4.6	> 33	1.0–4.3	2.4	17

Note: Depths: z1 = base of uniformly low chloride concentrations near the surface; z2 = depth of peak chloride concentration; z3 = upper limit of uniformly low chloride concentrations at depth, specific moisture flux, and number of samples from each borehole.

Table 4. Soil texture, volumetric moisture content, chloride concentration, $^{36}Cl/Cl$ ratios, ^{36}Cl concentrations in samples from borehole 51, and 3H ratios in samples from nearby borehole 52.

Depth (ft)	Soil texture	Moisture content (ft^3/ft^3)	g Cl / m^3 soil solution	Atoms $^{36}Cl/10^{12}$ atoms Cl	10^{12} atoms bomb $^{36}CL/m^3$ soil	Tritium (TU) (+8)
0.0–0.3	Loam	0.05	74.04	4.64+0.29	0.28	29
0.3–0.7	Loam	0.11	115.24	4.77+0.26	0.90	9
0.7–1.0	Loam	0.12	224.14	5.37+0.06	2.15	16
1.0–1.3	Clay loam	0.12	164.99	6.10+0.16	1.88	13
1.3–1.6	Clay loam	0.12	289.32	6.56+0.08	3.60	18
1.6–2.0	Clay loam	0.13	405.23	5.18+0.15	4.14	23
2.0–2.3	Silty clay loam	0.13	612.09	3.93+0.24	4.53	20
2.3–2.6	Clay loam	0.13	759.81	2.82+0.17	3.90	21
2.6–3.0	Silty clay loam	0.13	934.21	1.63+0.49	2.35	15
3.0–3.3	Clay	0.15	1193.46	0.93+0.38	1.30	0
3.3–4.1	—	—	—	—	—	22
4.1–4.9	—	0.15	2174.54	0.47+0.21	–0.19	28
4.9–5.7	—	—	—	—	—	15
5.7–6.6	—	0.08	2168.68	0.46+0.23	–1.21	8
6.6–7.4	Gravelly muddy sand	—	—	—	—	0

A dash indicates no data.

Table 5. Comparison of physical and chemical data from Texas, New Mexico, Nevada, Saudi Arabia, South Australia, and Cyprus.

	Texas[1] Hueco Bolson	New Mexico[2] SNWR1	New Mexico[2] SNWR2	New Mexico[2] NMSUR	Nevada[3] Yucca Wash	Saudi Arabia[4]	South Australia[5]	Cyprus[6]
Soil Texture	clay–loam to loam	fine sand	sandy loam	sandy loam	—	sand	—	—
Mean annual precipitation (in)	11.0	7.9	7.9	9.1	5.9	3.2	27.6–29.5	15.4
Moisture Content (ft^3/ft^3)	0.05–0.15	0.04–0.13	0.04–0.07	0.09–0.20	—	0.01–0.04	0.07–0.67	0.07
Water table depth (ft)	492	16	~ 330	~ 330	—	492	76–33	10
Water potential (MPa)	≥ –15.6	> –0.1	—	—	—	—	—	—
Chloride specific moisture flux (in/yr)	0.06	0.10	0.08	0.06	—	—	2.76–9.84	1.93–2.01
$^{36}Cl/^{35}Cl$ range Atoms $^{36}Cl/10^{12}$ atoms ^{35}Cl	0.5–6.6	0.1–17	0.7–5.9	0.5–20	—	—	—	—
$^{36}Cl/^{35}Cl$ peak depths (ft)	1.64	0.3–3.0	3.0	0.3, 2.3, 3.6	—	—	—	—
^{36}Cl specific moisture flux (peak depth) (in/yr)	0.06	0.12	0.10	0.10	0.07	—	—	—
^{36}Cl specific moisture flux (total penetration) (in/yr)	0.14	0.31	—	0.35	—	—	—	—
Total inventory 10^{12} atoms $^{36}Cl/m^2$	2.5	0.74	0.89	2.5	6	—	—	—
Tritium range (TU)	0–29	0–70	—	16–90	—	49–163	2–25	0–120
Tritium peak depths (ft)	0.0, 2.0, 4.6	0.3, 3.0, 6.2	—	1.0, 3.0, 4.6	—	1.5–14.1	1.0–28.9	32.8
Tritium specific flux (peak method) (in/yr)	0.28	0.33	—	0.37	—	0.91	2.0–1036	1.89

Sources: [1]this report; [2]Phillips and others (1988(; [3]Norris and others (1987); [4]Dincer and others (1974) [5]Allison and Hughes (1978); [6]Kitching and others (1980).

Note: a dash indicates no data.